ΙΔΡΥΜΑ ΤΕΧΝΟΛΟΓΙΑΣ ΚΑΙ ΕΡΕΥΝΑΣ

Foundation of Research and Technology Hellas

Institute of Molecular Biology and Biotechnology

&

University of Crete

Department of Biology

Master thesis comprised of:

Chapter I. Investigating the link between phase separation in RBP1 and its response to stress

Chapter II. Unraveling the role of Kin7.3 in blue light signaling

A thesis submitted for the degree of Master of Science
by

Vasiliki Katidou

Thesis Committee

Thesis supervisor: Associate Professor Panagiotis N. Moschou
Committee: Professor Kriton Kalantidis
Committee: Professor Michael Kokkinidis

October 2021

To the reader

At the beginning of my master thesis, two projects were proposed to me. As a result, my master thesis involves two separate projects and, thus, two different chapters.

Acknowledgements

I would like to sincerely thank Dr. Panagiotis N. Moschou for the opportunity to work in his lab, and the valuable guidance and support he provided throughout all of my academic experience as a master student and, hopefully, a budding researcher. Also, I would like to thank my colleagues phD students Andria Mentzelopoulou and Giannis Chatzianestis, but also Dr. Alexandra Delli for their help, whenever it was needed. Furthermore, I am thankful for the support and kindhearted banter from undergrad students Rafael Gkritzas, Stefanos Mastis, Irene Karapidaki, Ioanna Kiritsi, Haris Petritsopoulos and master students Anna Wulgarakis and Dafne Paraskeuopoulou, for making my everyday academic experience much more colorful.

Of course, I would like to make a special mention to master students Anastasia Fragkiadaki, which master thesis I followed as my academic “holy bible”, and Vasiliki Boumba, whose assistance in my master thesis was extremely helpful.

I would also like to thank Dr. Irene Dervisi, for the brief but meaningful academic encounter we shared. Last, but definitely not least, I would like to express my deepest respect, gratitude and admiration for Dr. Artemis Perraki, who guided me through all of my master thesis and was there for me, both professionally and personally. Artemis, none of this would be possible without you.

Thank you.

Chapter I. Investigating the link between phase separation in RBP1 and its response to stress

Abstract

Plant signaling responses can be triggered by diverse forms of abiotic stress, which are increasingly escalated by climate change. Therefore, deciphering how plants perceive and react to stress is becoming a highly necessary field of study. NtRBP1, a previously suggested to phase-separate in heat stress glycine-rich protein, provides a possible link between stress response and phase separation. The aim of my thesis was to investigate the properties of RBP1 that drive phase separation in stress response, employing (i) an *in silico* approach to assess its phase separation propensity and to identify possible post-translational modifications or disorder-to-order substitutions that disturb biomolecular condensation, (ii) a site-directed mutagenesis approach for the *in vitro* characterization of these predictions and (iii) a cell biology approach to uncover how phase separation is functionally linked to stress response and how it affects subcellular localization. My results showed that the predicted SUMOylation-deficient mutant RBP1^{K55R} did not show strikingly different subcellular localization patterns during heat and cold stress, nor it affected alternative splicing, but was successfully purified with RBP1 for further *in vitro* phase separation experiments. Additionally, *in silico* disorder prediction tools highlighted its phase-separation propensity and similarity to prion-like examples of amino acid composition. Finally, substitutions that alter predicted disorder-to-order (RBP1^{Y114F}) transition and phosphorylation site conservation (RBP1^{Y129F}), showed irregular subcellular localization patterns both in room temperature conditions and after heat stress, underlining the importance of further investigation for their functional impact. Overall, my findings provide insights to how phase separation and stress response are potentially linked, and highlight the importance of a more in-depth investigation of structural and functional changes in RBP1.

Κεφάλαιο Ι. Διερεύνηση της σχέσης της RBP1 με την αλλαγή φάσης σε συνθήκες καταπόνησης

Περίληψη

Οι μηχανισμοί σηματοδότησης των φυτών μπορεί να ενεργοποιηθούν από διάφορες μορφές αβιοτικού στρες, οι οποίες κλιμακώνονται ολοένα και περισσότερο από την κλιματική αλλαγή. Η NtRBP1, μια πλούσια σε γλυκίνες πρωτεΐνη που προηγουμένως είχε προταθεί πως προχωρά σε αλλαγή φάσης σε συνθήκες θερμικής καταπόνησης, προτείνει μια πιθανή σύνδεση μεταξύ της απόκρισης σε συνθήκες καταπόνησης και στο φαινόμενο αλλαγής φάσης. Ο σκοπός της διπλωματικής μου εργασίας ήταν να διερευνήσω τις ιδιότητες της RBP1 που προωθούν την αλλαγή φάσης σε συνθήκες στρες, ακολουθώντας (i) μια βιοπληροφορική προσέγγιση, για την εκτίμηση της τάσης προς αλλαγή φάσης και τον εντοπισμό πιθανών μετα-μεταφραστικών

τροποποιήσεων, αντικαταστάσεων ή μοριακών αλλαγών που οδηγουν από ασταθή σε σταθερή δομή και διαταράσσουν την αλλαγή φάσης (ii) μια προσέγγιση πρόκλησης σημειακών μεταλλάξεων για τον *in vitro* χαρακτηρισμό αυτών των προβλέψεων και (iii) μια προσέγγιση κυτταρικής βιολογίας, για να ερευνήσω πως ο διαχωρισμός φάσεων συνδέεται λειτουργικά με την απόκριση στο στρες και πώς επηρεάζει τον υποκυτταρικό εντοπισμό της RBP1. Τα αποτελέσματά μου έδειξαν ότι το μετάλλαγμα απώλειας σουμοϋλίωσης RBP1K^{55R} δεν προκάλεσε σημαντικές διαφορές στον υποκυτταρικό εντοπισμό σε συνθήκες θερμικής και ψυχρής καταπόνησης, ούτε επηρέασε το εναλλακτικό μάτισμα, αλλά απομονώθηκε μαζί με την RBP1 για μεταγενέστερα *in vitro* πειράματα. Επιπλέον, βιοπληροφορικές αναλύσεις υπογράμμισαν την τάση για αλλαγή φάσης και τη ομοιότητα της αμινοξικής της σύστασης με πράιονς . Τέλος, υποκαταστάσεις που δείχνουν μετάβαση από ασταθή σε σταθερή δομή (RBP1^{Y114F}) ή και επιπλέον συντηρημένες θέσεις φωσφορυλίωσης (RBP1^{Y129F}), έδειξαν ασυνήθιστα πρότυπα υποκυτταρικού εντοπισμού σε συνθήκες θερμοκρασίας δωματίου και θερμικής καταπόνησης, υπογραμμίζοντας την ανάγκη για περαιτέρω διερεύνηση της λειτουργικής τους επίδρασης. Συνολικά, τα αποτελέσματά μου παρέχουν περαιτέρω πληροφορίες για τον τρόπο με τον οποίο συνδέονται δυνητικά η αλλαγή φάσης και η απόκριση στο στρες, ενώ υπογραμμίζουν τη σημασία της βαθύτερης διερεύνησης των δομικών και λειτουργικών αλλαγών της RBP1.

Chapter II. Unraveling the role of Kin7.3 in blue light signaling

Abstract

Blue light (BL) photoreceptors are necessary components of signaling processes in plants, regulating the growth of plants to the most optimal position for survival and growth. Modern vertical farms utilize light-emitting diode lights with customized light to maximize efficiency, underlining the importance of deciphering the inner workings of BL response. My study aimed to contribute to the understanding of how Kin 7.3, a motor-based microtubule protein that was found to associate with BL photoreceptor PHOT1, is involved in blue light (BL) induced signaling response. Specifically, my thesis combined two approaches (i) genetic studies to explore the impact and the mechanism of PHOT1- dependent response to BL and (ii) cell biology experiments to study the effect of Kin7.3 on PHOT1 localization patterns and microtubule reorganization. Results showed that loss-of-function mutants display insensitivity to BL-induced bending, which poses a key phototropic response. Furthermore, PHOT1 distribution patterns at the plasma membrane (PM) appeared altered by the lack of Kin7.3, with PHOT1-GFP to present increased levels and retardation in internalization. Additionally, lack of Kin7.3 seems to affect microtubule BL-induced organization, with microtubules showing resistance to revert from a longitudinal to a transverse pattern of organization after BL-induced reorientation. Combined with experimental evidence suggesting that Kin7.3 affects the phosphorylation status of PHOT1, these assays collectively highlight Kin7.3 as a novel component of the PHOT1-dependent signaling.

Κεφάλαιο ΙΙ. Ο ρόλος της Κινεσίνης 7.3 στην απόκριση στο μπλε φως

Περίληψη

Οι φωτοϋποδοχείς μπλε φωτός είναι απαραίτητοι για τις διαδικασίες σηματοδότησης στα φυτά, ρυθμίζοντας την ανάπτυξη των φυτών για να επιτυγχάνουν τη βέλτιστη θέση για επιβίωση και ανάπτυξη. Σύγχρονες φάρμες παραγωγής χρησιμοποιούν συσκευές εκπομπής φωτός με προσαρμοσμένο φως για μεγιστοποίηση της απόδοσης, υπογραμμίζοντας τη σημασία της αποκρυπτογράφησης του μηχανιασμού απόκρισης στο μπλε φως. Η παρούσα διπλωματική εργασία στόχεψε στο να συμβάλει στην κατανόηση του τρόπου με τον οποίο η Κινεσίνη 7.3, μια πρωτεΐνη που κινείται πάνω στους μικροσωληνίσκους, βρέθηκε να σχετίζεται με τον φωτοϋποδοχέα του μπλε φωτός Φωτοτροπίνη 1 (PHOT1). Συγκεκριμένα, η διιπλωματική μου εργασία συνδύασε δύο προσεγγίσεις (i) γενετικές μελέτες για να διερευνήσει τον αντίκτυπο και τον μηχανισμό της απόκρισης της Φωτοτροπίνης 1 στο μπλε φως και (ii) πειράματα κυτταρικής βιολογίας, για να μελετήσει την επίδραση της Κινεσίνης 7.3 στα πρότυπα κυτταρικού εντοπισμού της Φωτοτροπίνης 1 και την αναδιοργάνωση των μικροσωληνίσκων. Τα αποτελέσματα έδειξαν ότι οι φυτικές σειρές με μεταλλάξεις απώλειας λειτουργίας δεν κάμπονται στο μπλε φως, που αποτελεί βασική φωτοτροπική απόκριση των φυτών. Επιπλέον, τα πρότυπα κατανομής της Φωτοτροπίνης 1 στην κυτταρική μεμβράνη παρατηρήθηκαν επηρεασμένα από την έλλειψη της Κινεσίνης 7.3 σε φυτικές σειρές PHOT1-GFP, παρουσιάζοντας αυξημένα επίπεδα έκφρασης στην πλασματική μεμβράνη και πιθανή καθυστέρηση στην ενδοκύτωση του υποδοχέα. Επιπλέον, η έλλειψη της Κινεσίνης φαίνεται να επηρεάζει την αναδιοργάνωση των μικροσωληνίσκων σε μπλε φως, ώστε να μην επαναφέρονται από ένα διαμήκη σε ένα εγκάρσιο πρότυπο οργάνωσης που προκαλείται από το μπλε φως. Σε συνδυασμό με πειραματικά στοιχεία που υποδηλώνουν ότι η Κινεσίνη 7.3 επηρεάζει την φωσφορυλίωση της Φωτοτροπίνης 1, τα αποτελέσματα αναδεικνύουν συλλογικά την συμμετοχή της Κινεσίνη 7.3 στην σηματοδότησης μέσω της Φωτοτροπίνης 1.

Chapter I. Investigating the link between phase separation in RBP1 and its response to stress

Introduction

Introduction -Chapter I

Biomolecular condensates -definition matters

Compartmentalization in biological systems is a key point in the spatiotemporal organization of signaling and has long been conventionally linked to membrane-bound organelles. Mitochondria, for example, contain a chemical environment necessary to make ATP[1], and lysosomes carry components necessary for the destruction of other proteins.[2,3] However, cells also harbor organelles that lack a delimiting membrane, held together via weak interactions between components and in a highly dynamic organizational state.[4,5] Hence, further sub-division and a local organization are established via non-membrane-bounded supramolecular assemblies, highly diverse in their physical properties, molecular compositions, subcellular locations, and functions -also known as Biomolecular Condensates.[6] They are reported to be composed of proteins, nucleic acids, and other molecular components within the nucleus (e.g., nucleolus, nuclear speckles) and the cytosol [e.g., stress granules (SGs), processing bodies, the centriole],[7] ranging in size from 20 nm (interchromatin granules) up to 1–6 µm (P granules) in diameter.[8,9] The protein components of condensates have been classified as either scaffold, which have been defined as the proteins that drive reversible condensate formation, or clients, proteins that preferentially partition into condensates.[10,11]

Liquid-liquid phase separation -the 'hows' and the 'whys'

Active formation and dissolution of these condensates are employed through liquid-liquid phase separation (LLPS) for many functions, such as stress response due to environmental stimuli[9,12], regulation of gene expression[13], or control of signal transduction.[14,15] Key parameters of LLPS are the concentrations of the molecular components (Figure 1A), the valency, and strength of interaction between molecules, the starting nucleation or seeding event (the biomolecular origin of LLPS) and changes due to environmental parameters such as ionic strength and pH, or thermodynamic parameters such as changes in temperature.[16] When solutions of macromolecules undergo LLPS, they condense into a dense phase that often resembles liquid droplets, and this dense phase coexists with a dilute phase (Figure 1B).[17] LLPS is driven through the exchange of macromolecule/water interactions for macromolecule/macromolecule and water/water interactions, under conditions that make this exchange energetically favorable.[18]

Non-strictly liquid -the space between us

Even though these biomolecular condensates are often referred to as liquids, some can also be solid, a liquid–gel, a solid–gel, a crystalline–solid, a semi-crystalline–solid, or liquid–crystalline, depending on local spatial ordering and preferred intermolecular orientations (Figure 1C). These two latter factors arise from hierarchies of interactions with different spatial extents and directional preferences, such as long-range electrostatics, multipolar interactions, hydrogen bonds, forces, and short-range interactions involving pi-systems[4], on which multiple bioinformatic

tools base their phase-separation prediction algorithms.[18] Multivalency can play an important role in three different conformations: (i) folded proteins, with well-defined interaction surfaces, can form oligomers with stereospecific interactions; (ii) folded domains can be associated through flexible linkers to generate linear multivalent proteins and (iii) intrinsically disordered regions (IDRs) can serve as scaffolds for multiple, specific linear motifs.[4,17,19]

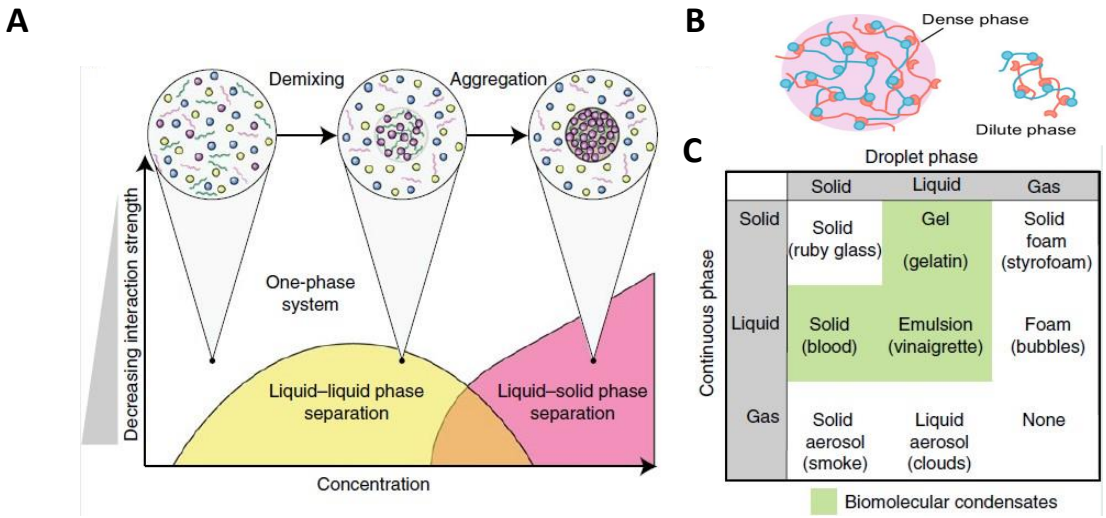

Figure 1. (A) Phase separation depends on multiple factors, including concentration, ionic strength, pH, macromolecular interactions and temperature[19], (B) Interchanging between a droplet and a dilute phase, which applies to droplets inside the nucleus and the cytoplasm[17], (C) Terminology and examples of biomolecular condensates, with liquid-liquid and liquid-solid considered most important for phase separation in biological systems.[19]

Truths and lies about IDRs

Traditionally, IDRs were considered to be passive segments in protein sequences that served as "links" for structured domains. However, it is now well established that IDRs can actively participate in diverse processes mediated by proteins.[20] IDRs affect the ability of proteins to fold into stable tertiary structures under physiological conditions, thus enabling them to swiftly interconvert between distinct conformations to serve their biological function.[21] A very recent study about Covid-19 underlines the biological implications of IDRs in LLPS, reporting that SARS-CoV-2 nucleocapsid (N) protein binds to the SG proteins such as GTPase-activating protein-binding proteins 1 and 2 (G3BP1/2), undergoing LLPS through its N-terminal intrinsically disordered region (IDR) with G3BP1 into SGs. [22] In terms of amino acid composition, IDRs often do not have many aromatic and aliphatic amino acids, which typically compose the core of folded domains, and do not adopt a single folded structure for the optimal single low-energy state. Instead, they could be punctuated by serine, glutamine, asparagine, and glycine (where glycine is counted with polar residues, because its properties are dominated by its polar backbone in the context of a protein), which phase separate homotypically *in vitro*.[23] These proteins assert a range of conformations with similar energies, determined by the primary sequence of the IDR.[24–26]

The importance of motifs -the case of RGG/RG

Arginine is a positively charged residue known to mediate hydrogen bonding and amino-aromatic interactions, and it is frequently found in protein motifs.[27] RGG motif and repeats are often clustered together with RG amino acids, implying that they may represent a single RGG/RG motif. RGG/RG repeats are usually found in three region types; low complexity regions, intrinsically disordered regions (IDRs) composed mainly of limited amino acid variation, or as part of intrinsically disordered proteins (IDPs).[28] The glycines in RGG/RG motifs likely contribute to the conformational flexibility for employing local structural elements necessary for RNA binding, also through pi-stacking with the peptide bond.[29–31] RGG/RG repeats have also been shown to mediate protein-protein interactions and to be crucial for the recruitment of proteins to multiple types of membrane-less organelles or biological condensate.[32–34] Arginine and glycine provide unique properties to associate with phase separation [35], both having the potential to form long-range pi-pi stacking interactions, an interaction module that can be used to predict phase separation propensity.[34]

Sequence- it's not always bad to be 2D

Despite little conservation in amino acid sequence alignments, IDRs share sequence-distributed molecular features, such as biophysical properties, repeats, and short linear motifs, likely due to natural selection and linked to biological importance.[36,37] Every different protein conformation, as a result of the IDR domain, can result in specific binding activities and properties for its partner.[38] Approximately two-thirds of IDRs structurally solved adopt a distinct secondary structure[39], without excluding that some surfaces retain flexibility of dynamism, even when bound.[40,41] Perturbations of conditions that affect cell state can modulate the optimal conformation, thus indirectly control protein-protein interactions without the direct mode of conventional interfacing, shown through various examples.[42–44]

Proteins and RNA- the value of bonding

Protein-protein networks are dynamic, organized into functional nodes or hubs.[45] In humans, approximately 30% of these hubs contain RNA-binding proteins (RBPs), which in turn contain disordered motifs.[46] The formation of these hubs is highly correlated with IDRs in proteins.[47] One potential function of biomolecular condensates is RNA synthesis, processing, metabolism, expression, and silencing in different subcellular locations, mediated at least in part by RNA Binding Proteins (RBPs) contained within them.[9,48–51] RNA-binding proteins (RBPs) are essential chaperones that interact with RNA via one or multiple globular RNA-binding domains (RBDs).[52] RBPs are important regulators of all steps of the mRNA life cycle, such as transcription, pre-mRNA processing, localization, translation, and decay, therefore highly impacting gene expression patterns. This, in turn, can affect cell fate determination, tissue identity, and organism development[53], since specific RBPs that harbor mutations are reported to cause severe phenotypes or lethality.[54] The functional characteristics of RBPs indicate that a variety of RNA-binding domains (RBDs) facilitate direct interactions between RBPs and their target mRNAs.[55]

RRM -thinking inside the box

RBDs include various motifs, such as the RNA recognition motif [RRM, also known as RBD or ribonucleoprotein (RNP) domain], the hnRNP K homology (KH) domain, the zinc finger motif, the pentatricopeptide repeat (PPR) motif, Asp-Glu-Ala-Asp (DEAD) boxes, Pumilio/FBF (PUF) domains, and the double-stranded RNA binding domain (dsRBD).[56–59] The RRM was originally reported in the late 1980s, when it was shown that mRNA precursors (pre-mRNA) and heterogeneous nuclear RNAs (hnRNAs) constantly form complexes with proteins [60], an abundant motif in all life kingdoms, mainly in eukaryotes but also found in prokaryotes and viruses.[61] The RRM domain is approximately 90 amino acids in length, harboring a central, conserved sequence of eight residues consisting of mainly aromatic and positively charged amino acids, specifically Lys/Arg-Gly-Phe/Tyr-Gly/Ala-Phe/Tyr-Val/Ile/Leu-X-Phe/Tyr, where X can be any amino acid.[62,63] Further studies revealed another, less conserved consensus sequence, Ile/Val/Leu-Phe/Tyr-Ile/Val/Leu-X-Asn-Leu, establishing these different motifs as RNP1 and RNP2, respectively.[64] RRM folds into four β- strands and two α-helices, while the surface area of the β-sheet is responsible for the RNA interaction. The β1 strand contains the conserved hexapeptide RNP2 (ribonucleoprotein consensus sequence 2) and the β3 strands the highly conserved octapeptide RNP1.[65]

GRPs -Rich but in Glycine

Glycine-rich proteins (GRPs) are involved in abiotic and biotic stress response, distinguished by their high glycine content (up to 70%), with repetitive amino acid distributed motifs.[66] GRP-encoding genes are commonly found in many eukaryotic species.[67] Glycine-rich GRP-1 from *Petunia hybrida* was the first identified protein of this superfamily, with 252 out of 384 total amino acids glycine residues. The highly variable expression and subcellular localization patterns of these GRPs indicate that these proteins are main actors in various physiological processes, not just cell wall plasticity as they were originally described. [59,68] Based on domain features, the GRPs can be

GRP classes	Characteristic features
Class I	Signal peptide followed by high glycine-content region with $(GGX)_n$ repeats
Class II	Signal peptide and presence of a characteristic cysteine-rich C-terminal domain
Class III	Signal peptide and contain lower glycine content (in comparison to other GRPs classes), the oleosin domain is the signature motif for their sub-group
Class IV	RNA-binding GRPs, glycine-rich domain with RNA-recognition motif (RRM) or a cold shock domain (CSD), CCHC zinc-fingers might be also present in their structure, four sub-groups: (**IVa**) RRM motif besides the glycine-rich domain, (**IVb**) single RRM and CCHC zinc-finger motif, (**IVc**) cold shock domain and two or even more zinc-fingers, (**IVd**) two RRM motifs
Class V	Signal peptide followed by GGX/GXGX motif or only GGX/GXGX motif without signal peptide

Figure 2. Summary of glycine-rich protein classes, based on their structural properties. Reprinted by Czolpinska, M. and Rurek, M. [58]

divided into five classes [69], although others differentiate them into four.[67] Class I–III GRPs share typical N-terminal signal peptides, although featuring different motifs in their glycine-rich domains. Class IV of GRPs feature nucleic acid-binding domains, most of which are RNA-binding domains.[70] Specifically, the RRM in Class IV functions in transcription and post-transcriptional modifications, thereby regulating multiple metabolic pathways.[61,71] A different set of GRPs with a high glycine content but mixed patterns of repeats from eucalyptus[72] and other genomes proposes the introduction of a new class of GRPs (Class V) (Figure 2).

Post-translational modifications -Lost in post-translation

Post Translational Modifications (PTMs) modulate critical biological processes such as protein signaling, localization, and degradation[73], characterized as additions of functional groups (e.g., phosphoryl, methyl, acyl, glycosyl, alkyl, etc.) or subtler chemical changes such as oxidation, deimidation, and deamidation that alter the physical or chemical properties of amino acids.[74] Arginine methylation and serine, tyrosine, and serine/threonine phosphorylation are the most well-studied PTMs that adjust phase separation of RBPs. Arginine methylation impairs phase separation by reducing cation–pi interactions between arginine and aromatic amino acids.[13,75,76] Other PTMs, including PARylation, ubiquitination, lysine acetylation, SUMOylation (from SUMO, Small Ubiquitin-related Modifier), and O-linked GlcNAcylation have been linked to phase separation in other proteins and may also impact RBPs.[16,77,78]

SUMO -wrestling inside the cell

SUMO is reportedly involved in regulating a wide variety of proteins in many pathways and it can regulate protein function beyond degradation.[79,80] Proteomic studies have identified more than 1000 target proteins in the Arabidopsis proteome, shedding light on the pivotal role of this PTM.[81] In plants, SUMO has been linked to various biological processes, such as DNA repair, chromatin modification/remodeling, transcriptional regulation, RNA metabolism, growth, flowering, light

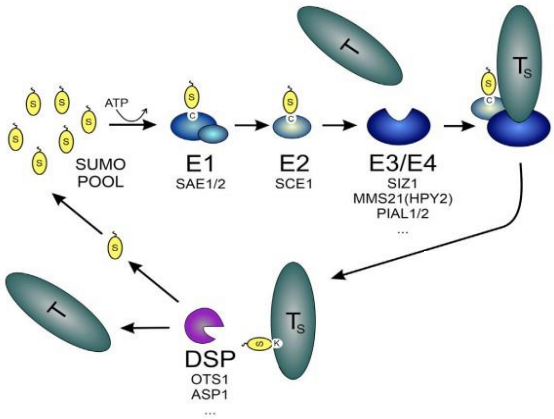

Figure 3. Simplified representation of the SUMO machinery and cycle. SUMO modules (S) are activated by the E1 enzyme SAE1/2 heterodimer, by hydrolyzing ATP. SUMO is transferred to the E2 enzyme SCE1, enabling target protein (T) recognition together with the E3 enzyme. The SUMOylated target protein is post-translationally modified, but can also be reversely modified by deSUMOylating proteases (DSP). Detached SUMO re-enters the SUMO pool of the cell. SAE1/2, SCE1, SIZ1, MMS21 and PIAL1/2 stand for the Arabidopsis homologs of the SUMO conjugation enzymes and OTS1, ASP1 for DSPs. Adapted from Zeilder. [89]

signaling, abiotic stress responses, and responses to pathogen infection.[82–88] SUMO-specific enzymes attach SUMO enzymes in an ATP-dependent manner, commencing an enzymatic cascade that resembles ubiquitylation.[89] Approximately 60% of Arabidopsis proteins share the SUMO consensus motif (cKxE/D; c a large hydrophobic amino acid residue; K, the acceptor lysine; x, any amino acid; E/D, glutamate or aspartate), although multiple targets identified in proteomics studies were SUMOylated at non-consensus sites.[81]

SUMO -inside or outside the nucleus 'ring'

Insights into biomolecular condensates suggest that SUMO's ability to facilitate protein-protein interactions can contribute to phase separation[3], while also data from modeling SUMO:SIM (SUMO Interacting Motif) interactions in engineered proteins present the sufficiency of this PTM for driving phase separation *in vitro*.[11] Promyelotic leukemia (PML) nuclear bodies (NBs), for example, are an archetype of membrane-less organelles that concentrate proteins at shell-like structures within the nucleus, thought to be followed by multivalent SUMO–SIM interactions of the PML scaffold and partner proteins, thus forming biomolecular condensates.[90,91] Cytoplasmic SUMOylation of a target protein may also inhibit its nuclear import. For example, in the case of c-Myb (transcription factor), cytosolic c-Myb is found solely SUMOylated, while nuclear-localized c-Myb is found in unmodified form.[92] In another example, the transcription factor ATF7 is regulated by SUMOylation and presents subtle effects in the rates of nuclear import.[96]

Alternative splicing -it's ok to be different

The regulation of alternative splicing (AS) of thousands of genes plays a central role in determining the phenotype of a cell. During splicing, 5' and 3' splice sites, serving as borders of introns in a pre-mRNAs, coupled with the branch site (a consensus sequence residing near the 3' splice site) are recognized by various proteins associated with well-characterized noncoding RNAs (Uridine-rich small nuclear RNAs or snRNAs). The spliceosome, a large molecular complex, is assembled sequentially by five small nuclear ribonucleoproteins (snRNPs) (U1, U2, U4, U5, and U6) and their associated proteins (snRNP).[93] Amongst the developmental and physiological

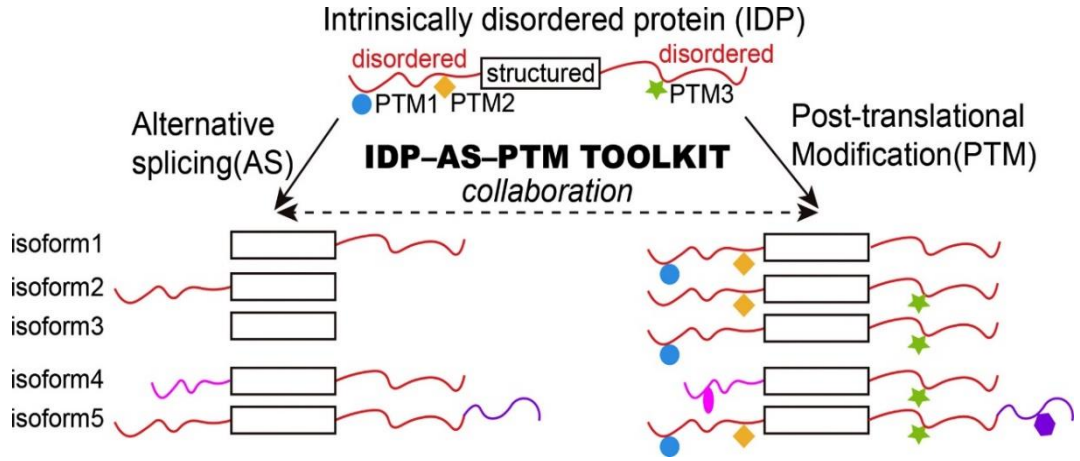

Figure 4. IDPs collaborate with AS and PTMs to produce an IDP-AS-PTM toolkit. This proposed toolkit is valuable in complex context-dependent cell signaling and regulation. Reprinted from Zhou et. al. [100]

strategies that plants employ to retain their developmental plasticity and respond to diverse conditions, AS produces multiple mRNAs from the same gene, through the variable selection of splice sites or retention of introns during precursor-mRNA (pre-mRNA) splicing.[94] The proteomic-mediated identification of RBPs as the predominant group among SUMO conjugation targets underlines the importance of this PTM at distinct steps of mRNA metabolism.[95,96] Combined with the phase-separation propensity of IDRs and SUMOylation, AS could be linked in a wider IDP-AS-PTM system that addresses the complexity of cell signaling and regulation (Figure 4).[97]

AtGRP7 -slavery is not dead yet

Regulation of AS in different cell types and under different conditions depends on sequence elements in pre-mRNAs and the interactions of RBPs, which differentiate in terms of concentration and activity.[94] There is no simple division of positive and negative splicing regulators, as this behavior frequently depends on the location of the binding site relative to the regulated exon, or even the protein levels of specific RBPs. A prime example of the latter, AtGRP7, is a GR-RBP that autoregulates its expression and plays a key role in splice site selection within the *AtGRP8* transcript, favoring the production of an alternatively spliced, unstable transcript.[98] By forming a negative feedback circuit, AtGRP7 undergoes circadian oscillations, proposing a "slave" oscillator in *Arabidopsis* that receives temporal information from a central "master" oscillator, retains the rhythmicity by negative feedback, and feeds it to the output pathway by regulating a subset of clock-controlled transcripts. [99] *At*GRP7 has been extensively studied for its functional impact on various processes, such as abiotic[100–102], biotic response[103], regulation of circadian rhythm [98,99,104], but also post-translational modifications responsible for its effect on AS via the RALF1-FER pathway.[105] FERONIA (FER) is a receptor-like kinase (RLK) that functions as a versatile signaling receptor for the rapid alkalinization factor (RALF) peptides (e.g., RALF1 and RALF23). FER binds to RALF and becomes autophosphorylated, acting in an inhibitory manner for the plasma membrane H^+-ATPase activity, increasing apoplastic pH, and reducing cell elongation.[106] The phosphorylation AtGRP7 by RALF1-FER signaling alters the RNA binding ability of AtGRP7 and results in changes to AS patterns.

GR-RBP1 and AtGRP7- we're more alike than you think

Nicotiana tabacum GR-RBP1 is highly similar to *At*GRP7, a ∼16 kDa protein that contains an RRM domain (85 residues), followed by a glycine-rich region of roughly the same length.[107] Sequence alignment shows that NtGR-RBP1 is highly conserved, with orthologous in Arabidopsis and Zea mays sharing 76% and 73% amino acid identity, respectively, and ∼40% homology evident to its mouse, human, and bacterial counterpart (Figure 5). Similarly to the involvement of AtGRP7 in stress responses, the levels of Nt-RBP1 mRNA were found upregulated in response to cold stress, modulated in salt stress, while wounding caused no apparent effect.[108] Also, NtGR-RBP1 was reported as an RNA chaperone in melting nucleic acid assays [107], thus a protein that instructs the proper folding of the misfolded target RNAs and further rescues the translation under cold stress. [109]

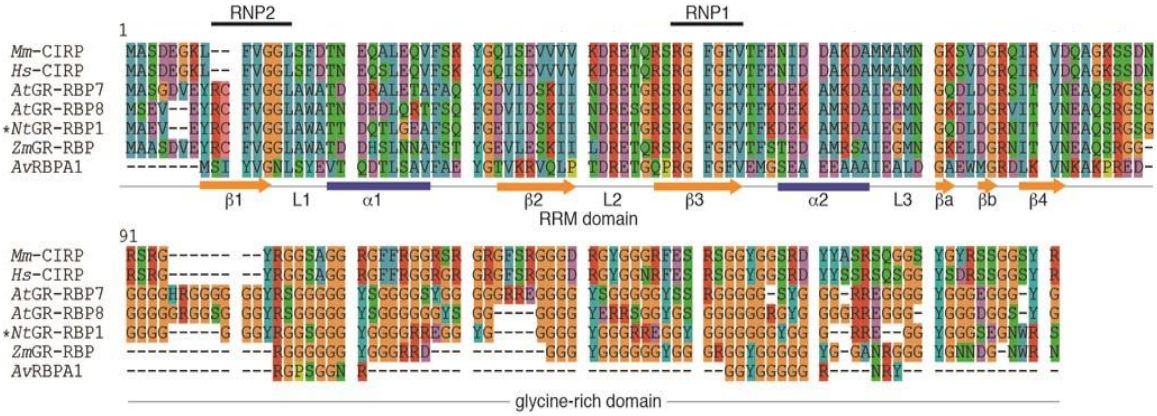

Figure 5.Protein sequence alignment and conservation analysis of NtGR-RBP1 homologs in Arabidopsis, M.musculus, H.sapiens and Z.m, showing high conservation level from bacteria to human. The alignment is generated by CLUSTAL W and displayed by Seaview with colour coding according to amino acid properties. The location of the RNP motifs and the glycine-rich region is indicated. Secondary structure elements as present in the structure of the NtRRM domain of NtGR-RBP1 are indicated below the alignment (orange arrows: β-strand; blue bars: α-helix). GR-RBP = glycine-rich RNA-binding protein; RBP = RNA-binding protein. Adapted from Khan et.al. [114]

GR region -I want to break free

The glycine-rich region of NtRBP1 appears to mediate intermolecular self-association with the RRM domain, while NMR RRM resonances are severely broadened and displaced in the context of full-length NtGR-RBP1.[107] This proposes a continuous interchange between free and GR-bound states of the RRM domain, with the GR region exchanging conformations in between a fully unfolded and a structured polypeptide, akin to a molten globule. A small number of arginines distributed within the GR sequence raises the question of whether they could be considered as RGG/RG motifs and, thus, affect the conformational properties of RBP1 in this context-dependent manner. A similar percentage of tyrosines (Y) in the GR tail with arginines (R) proposes an additional type of region, the GYR region.[107] Studies of AtGR-RBP7 nuclear localization show that the GR region facilitates transportin-mediated nuclear import[110], which could also be functionally applied for the proposed GYR region of NtGR-RBP1.

Aim of study -Chapter I

The aim of my thesis was to investigate the link between phase separation and stress response in RBP1. This work is built on preliminary results from Dr. Moschou's lab, suggesting that RBP1 shows phase-separation properties in heat stress. However, the mechanisms that promote phase separation remain elusive. Therefore, I followed:

(i) an *in silico* approach to predict phase-separation propensity and possible alterations in RBP1

(ii) an *in vitro* site directed mutagenesis approach to apply the predicted *in silico* changes

(iii) a cell biology approach to assess the functional and subcellular localization impact of mutated RBP1

Results -Chapter I

Previous work in Dr. Moschou's lab generated transgenic *N.tabacum* RBP1 (overexpressors 35S::RBP1) and knockout (CRISPR) lines and characterized their phenotypes in growth and abiotic response. Overexpression lines of RBP1 show a 'greener' phenotype and early flowering (unpublished data and Karapidaki[111]). NtRBP1 is phylogenetically related to the Arabidopsis cold-stress response related GRP7 protein, with a high degree of homology according to ClustalW[112] (Figure 6A), pointing to its possible involvement in mediating stress response. Preliminary results of fluorescently tagged, transiently expressed in *N.benthamiana* 35S::GFP-RBP1 showed that RBP1's function is possibly regulated through phase separation (Figure 6B). It was also demonstrated that RBP1 relocalized more prominently to the inside of the nucleus upon stress responses (unpublished data). Phase separation of proteins is often linked to PTMs that might change their material properties and/or interaction partners.[73] SUMOylation is a prominent biological mechanism in protein regulation, while several examples pointing to its impact in phase transitions of proteins.[3]

By assessing these previous observations and based on existing literature on phase separation, I aimed to investigate whether this PTM is involved in the phase separation properties of RBP1. By implementing the SUMOylation prediction tool SUMOgo[113], I discovered NtRBP1 Lysine 55 as a putative site of possible SUMOylation (Figure6A). However, it is important to note that Lysine 58 was also predicted as the second most probable putative SUMOylation site (out of two results), albeit with a much lower score (K58=0.16 versus K55=0.44). Therefore, I decided to follow a targeted mutagenesis approach on NtRBP1, by selecting K55R as a possible candidate for SUMOylation and investigate its possible effect in phase separation inhibition or negation of nuclear localization.

To investigate the effect of K55R, I performed site-directed mutagenesis (Supplemental figures, S1A), introducing a point mutation in position 55 and substituting Lysine with Arginine, which creates a 'SUMO-dead' mutant due to the lysine-to-arginine conservative substitution.[114] Afterwards, I transiently expressed in *N.benthamiana* epidermal leaves fluorescently labeled 35S::GFP-RBP1 and 35S::GFP-RBP1^{K55R} and compared their localization patterns by confocal imaging at 96h post-infiltration (Figure 6C), with the valuable help of Dr. Moschou in the imaging capturing process. First, we observed that, when samples were exposed to room temperature (RT) conditions, both GFP-RBP1 and GFP-RBP1^{K55R} showed droplet formation in leaf epidermal cells, possibly due to mechanical stress by the placement of coverslip above the specimen (Figure 6C, top). Supportive evidence of this finding was the time course experiments analysis by collaborators, which showed RBP1 droplet formation induced by mechanical stress. Collectively, these data suggest that RBP1 might be involved in a wider spectrum of stress-related responses.

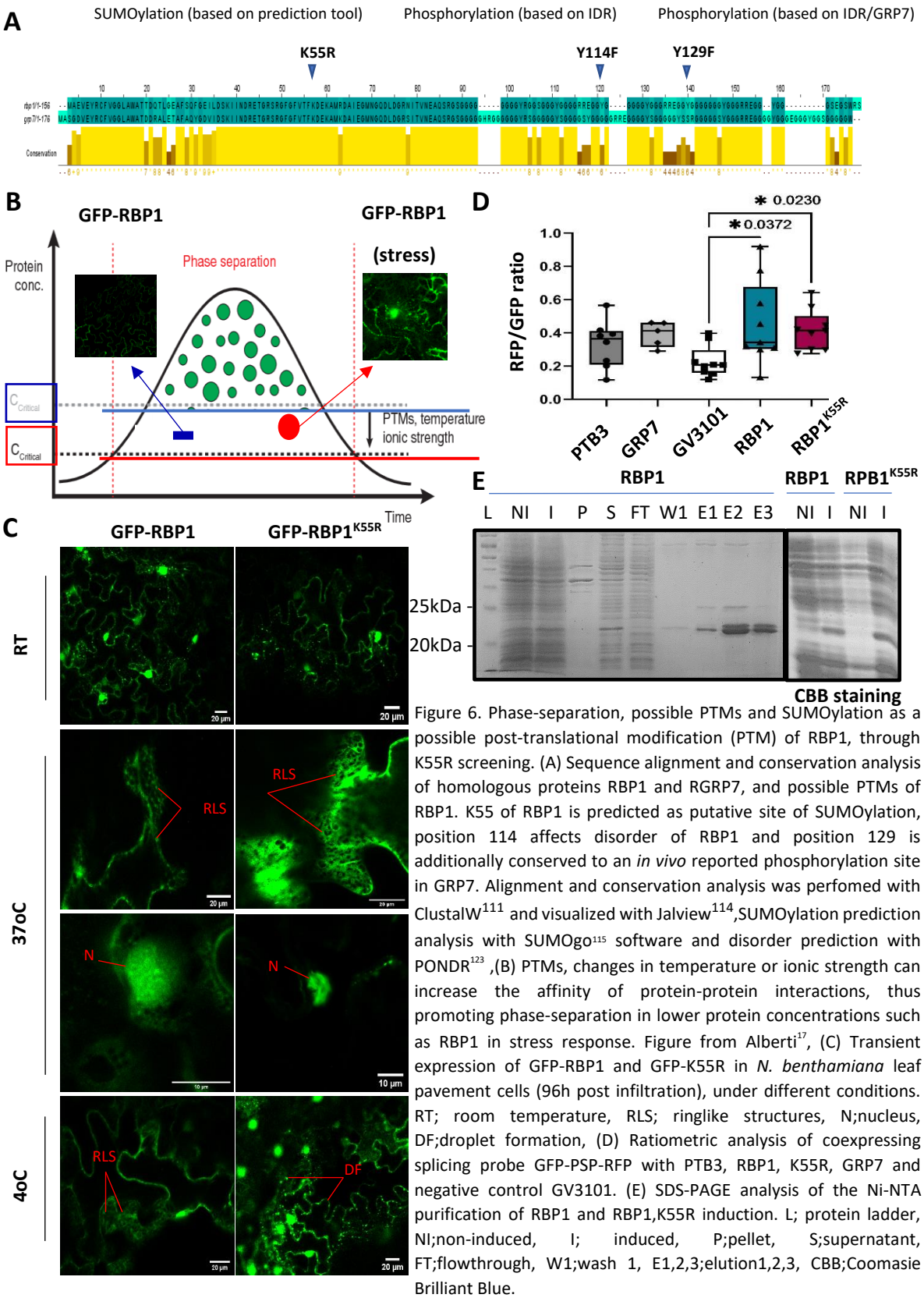

Figure 6. Phase-separation, possible PTMs and SUMOylation as a possible post-translational modification (PTM) of RBP1, through K55R screening. (A) Sequence alignment and conservation analysis of homologous proteins RBP1 and RGRP7, and possible PTMs of RBP1. K55 of RBP1 is predicted as putative site of SUMOylation, position 114 affects disorder of RBP1 and position 129 is additionally conserved to an *in vivo* reported phosphorylation site in GRP7. Alignment and conservation analysis was perfomed with ClustalW[111] and visualized with Jalview[114],SUMOylation prediction analysis with SUMOgo[115] software and disorder prediction with PONDR[123] ,(B) PTMs, changes in temperature or ionic strength can increase the affinity of protein-protein interactions, thus promoting phase-separation in lower protein concentrations such as RBP1 in stress response. Figure from Alberti[17], (C) Transient expression of GFP-RBP1 and GFP-K55R in *N. benthamiana* leaf pavement cells (96h post infiltration), under different conditions. RT; room temperature, RLS; ringlike structures, N;nucleus, DF;droplet formation, (D) Ratiometric analysis of coexpressing splicing probe GFP-PSP-RFP with PTB3, RBP1, K55R, GRP7 and negative control GV3101. (E) SDS-PAGE analysis of the Ni-NTA purification of RBP1 and RBP1,K55R induction. L; protein ladder, NI;non-induced, I; induced, P;pellet, S;supernatant, FT;flowthrough, W1;wash 1, E1,2,3;elution1,2,3, CBB;Coomasie Brilliant Blue.

Next, we found that heat stress treatment (37°C, 30min) induced the formation of ring-like GFP-NtRBP1 structures (Figure 6C, upper middle), reminiscent of ER-PM contact sites.[115] Major differences were not distinguished regarding the formation of the ring-like structure between WT and RBP1^{K55R}. However, we found that GFP-RBP1 formed prominent condensates inside the nucleus (Figure 6C, left lower middle). Additionally, we came across an uneven pattern of GFP-RBP1^{K55R} nuclear distribution (Figure 6C, right lower middle). Since stress response is a well-known trait of homologous *AtGRP7*[116], we also tested how GFP-RBP1 and GFP- RBP1^{K55R} respond to stress. Results show that cold stress promotes ring-like structure formation of GFP-RBP1, with some mesh-like array points that could reflect a possible association with Golgi apparatus[117](Figure 6C, bottom left). Interestingly, we observed more pronounced droplet formation in GFP-RBP1^{K55R}, especially close to the PM (Figure 6C, bottom right).

To discover the effect of RBP1 in transcriptome regulation, RNA-seq analysis was previously performed in Dr. Moschou's lab using the overexpressors and CRISPR RBP1 lines (unpublished data, Dr. Moschou's lab). Results showed that RBP1 is involved in AS, particularly favoring 3' splice sites. Since RBP1^{K55R} seems to affect protein propensity for phase separation to some degree, my next goal was to investigate whether K55R affects RBP1 function in alternative splicing. Thereby, I performed a ratiometric assay by employing a splicing probe that was designed inside the lab (Supplemental Figures, S1B). The design is based on the exon skipping properties of PTB3 with a substrate, namely PSP in design, featuring a GFP-tag and an RFP-tag flanking PSP on the left and right border, respectively. PSP contains an exon (exon2) with a stop codon that, when it is alternatively spliced, promotes the expression of RFP-tag and the diminution of the GFP signal compared to the complete absence of alternative factors, due to partial alternative splicing. Thus, ratiometric calculation of the two fluorescent tags is predicted to indicate the exon-skipping levels in the cells.

Using the aforementioned splicing probe, I performed a similar experiment using PTB3, GRP7 (both known to be involved in alternative splicing, albeit in specific conditions) [105,118], RBP1, RBP1^{K55R,} and empty Agrobacterium (GV3101) as a negative control. Then, I compared the effect of RBP1 and RBP1^{K55R} in alternative splicing. My results showed that the presence of these constructs caused statistically significant differences in the RFP/GFP ratio compared to the negative control GV3101, illustrating that both RBP1 and RBP1^{K55R} can induce exon skipping (Figure 6D & Supplemental Figures, S1C). Yet, RBP1^{K55R} appears to promote alternative splicing similarly to RBP1. Collectively, to test the effects of the splicing probe, further repeats of this assay are necessary for more clear conclusions.

To show that a protein can phase separate, it is important to perform further *in vitro* experiments based on literature guidelines.[18] Therefore, I purified recombinant RBP1 and RBP1^{K55R} from bacterial cultures, useful for future *in vitro* phase separation assays. In further detail, I inserted RBP1 and RBP1^{K55R} into a PGAT4 vector (T7 promoter), suitable for bacterial expression, and performed Immobilized Metal Affinity Chromatography (IMAC) using Ni beads. Both constructs were expressed in *E.coli* cultures and induction of protein expression with IPTG was initiated at OD~0.6, in 28°C for 3 h. SDS-page showed that RBP1 (Figure 6E) and RBP1^{K55R} (Supplemental

Figures, S1D) were both located in the supernatant soluble fraction and were successfully eluted (E2,E3) in large quantities and good levels of purity. When expressed in bacterial cells, RBP1 showed an unexpected electrophoretic shift to higher molecular weight (~22kDa instead of 16kDa), possibly due to the high Glycine content that interferes with SDS mediated denaturation.[119] Future experiments will involve the analysis of single protein RBP1 and RBP1^{K55R} properties in presence of different buffer conditions, following recent protocols established in the lab.

Although the structural information of whole protein is still elusive, the RNA-binding domain of *N. tabacum* RBP1 has been characterized through NMR analysis before[107] and the K55 resides inside this domain (Figure 7A, top). Further structural characterization is inhibited by the intrinsically disordered glycine-rich domain at the tail region of RBP1. To gain further insight on RBP1 structure and function, I performed *in silico* analysis of phase separation predictions for RBP1. Pi-pi interactions between (but not strictly) aromatic rings are important for promoting phase separation[120] and Pi-pi prediction tool[30] places the glycine-rich region of RBP1 above the threshold P score, highlighting the intrinsically disordered propensities of the protein (Figure 7A, upper left). Protein state diagram prediction by CIDER[121] places RBP1 close to the Janus sequences area, further supporting *in silico* predictions that RBP1 phase separates (Figure 7A, middle). A comparative analysis of RBP1 amino acid sequence with prion-like proteins or domains shows that RBP1 shares a composition bias similar to prion-like proteins (Figure 7, bottom). Taken together, these results support the intrinsically disordered properties of RBP1 by sequence and amino acid group analysis, which could drive phase separation and its specific functions in stress.

Another useful disorder prediction tool is PONDR, which functioned as the first tool designed specifically for the prediction of protein disorder.[122] Substitution of Tyrosine (Y) with Phenylalanine (F) appeared to change the disorder status of the protein in position 114 (Figure 7C, square) and 129 (Supplemental Figures, S1E,F). Based on such IDR predictions, I introduced two single, individual conservative mutations of Tyrosine (Y) to Phenylalanine (F) at the positions Y114 and Y129 (Figure 6A), expected to alter the IDR properties of RBP1 and aimed to examine its effects on phase separation. Interestingly, a recent paper showed that GRP7, the close homolog of RBP1 in *A.thaliana* is activated through its phosphorylation by the receptor kinase FERONIA at the position S139[105], while Y129 of RBP1 is located in a conserved position with GRP7-S139.

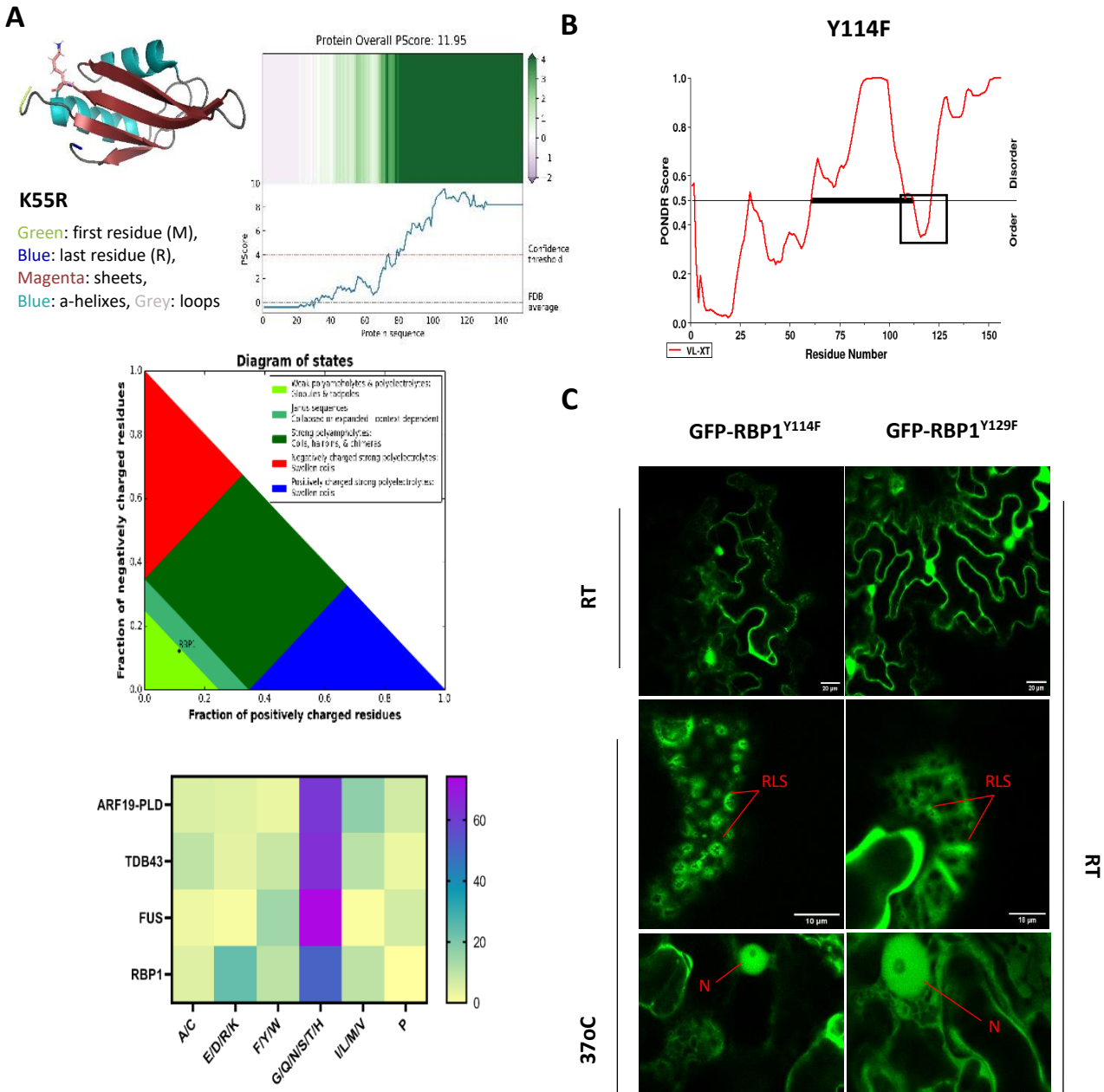

Figure 7. Phase-separation and structural properties of RBP1, Y114F and Y129F. (A) (upper) Structure solution of RNA-binding domain of RBP1 and highlighted K55[109] , (middle) Pi-pi interactions of RBP1 aminoacids show positively predicted phase-separation and protein state diagram places RBP1 close to collapsed/expanded state. Prediction by Pi-Pi[29] and CIDER[123] respectively, (lower) Comparative analysis of RBP1 in relation to different proteins with prion-like properties. PLD composition in relation to different proteins. Each amino acid is assigned to one of six groups on the x axis, and the fractional difference of grouped amino acids between RBP1 and each sequence is shown, (B) Evaluation of intrinsic disorder with PONDR[124] VLXT shows the transition from disorder to order with Y114F substitution, (C) Transient expression of GFP-RBP1^{Y114F} and GFP-RBP1^{Y129F} in *N. benthamiana* leaf pavement cells (96h post infiltration), under different conditions. RT; room temperature, RLS; ringlike structures, N;nucleus, AAG;aggregates.

Following the same point-mutation pipeline for K55R, I investigated the localization patterns of RBP1^{Y114F} and RBP1^{Y129F} by transient expression in *N.benthamiana* and confocal microscopy. Both mutants showed nuclear localization in RT (Figure 7D, top). Concerning the GFP-RBP1^{Y114F} mutant, heat stress produced more concentrated ring-like structures (Figure D, left upper middle), homogenous distribution in the nuclear compartment (absence of puncta) (Figure 7D, left lower middle), and irregular aggregates (Figure 7D, bottom left). The aggregates were observed in some, but not all samples and could be related to the disorder-to-order transition of droplets to their stabilization to aggregates.[123] Our analysis also showed that, while the RBP1 and K55R mutant presented nuclear localization (Figure 7C) in RT and ring-like structures during heat stress, the RBP1^{Y129F} presented ring-like structures in RT (Figure 7, right upper middle). Additionally, following heat stress, we observed a mostly cytoplasmic localization of the GFP-RBP1^{Y129F}, with few droplets dispersed inside the leaf pavement cells (Figure 7D, bottom right). A more uniform distribution (fewer puncta) of GFP- RBP1^{Y129F} was observed inside the nucleus (Figure 7C, right lower middle).

Overall, we conclude that the GFP-RBP1^{Y114F} and GFP-RBP1^{129F} mutants present distinct localization patterns in RT and stress response conditions, possing questions about the specific impact of these substitutions in RBP1 function. For instance, the impact of these substitutions in the role of RBP1 in alternative splicing is highly relevant for future studies. Despite results suggesting that RBP1 is a general stress response protein in comparison to cold-stress related GRP7, more experiments are necessary to elucidate the functional role, the phase separation properties, and the effect of PTMs regarding RBP1.

Discussion

Plant stress responses are comprised of molecular and cellular processes that are triggered by diverse forms of stress and limit the distribution, growth, and development of plants.[124] Regarding the adverse effects of abiotic stresses, exacerbation of stress parameters due to climate change is predicted to lead to an increased frequency.[125] Unraveling the roles and functions of stress response proteins is becoming a more and more necessary field of study and RBP1 is involved in a seemingly wide spectrum of stress stimuli. AtGRP7, also known for showing increased expression induced by cold stress, is a close homolog of NtRBP1 (Figure 6A). In *N. tabacum*, transgenic lines of 35S::RBP1 and CRISPR *rbp1* lines show a 'greener' phenotype and early flowering, the latter of which is an indicator of stress.[126] Preliminary results in Dr. Moschou's lab have shown more nuclear localization of RBP1 during heat stress, while also transient expression of GFP-fused RBP1 displays droplet formation as a general response to stress stimuli (Figure 6B).

PTMs, especially SUMOylation, are reportedly involved in phase separation.[79] RBP1 K55 was selected according to the results obtained by the *in silico* prediction tool SUMOgo[113] and GFP-RBP1 and GFP-RBP1^{K55R} were investigated side-by-side by performing site-directed mutagenesis. Transient expression of these two constructs did not show major differences in the subcellular distribution in RT (Figure 6C, top), but heat stress produced ring-like structures (Figure 6C, upper-middle) and seemed to favor GFP-RBP1 nuclear distribution compared to uneven GFP-RBP1^{K55R} distribution inside the nucleus (Figure 6C, lower middle).

In contrast, cold stress produced the same ring-like structures in GFP-RBP1 (Figure 6C, bottom left) and induced droplet formation in GFP-RBP1^{K55R}. RBP1^{K55R} was able to show liquid-liquid phase separation properties through droplet formation during cold stress, which is contradictive to the temperature-dependent threshold that usually favors higher temperatures for phase separation of proteins. However, a possible interactor that associates with RBP1 more optimally during cold stress could be responsible for droplet formation or due to cytoplasmic immediate rise in cytosolic free calcium concentration ([Ca2+]cyt)[127] that impacts droplet formation due to electrostatic forces. Further examination is required to distinguish between the effect of this substitution in a cell biology aspect and temperature effects in phase separation properties of a protein that is homologous to cold-induced GRP7. Furthermore, mass spectrometry analysis is in progress, to give some insight into possible interactors of RBP1.

RNA-seq analysis from Dr. Moschou's lab has shown that RBP1 is probably involved in AS, especially favoring the 3' splice site (unpublished data). By using the splicing probe that was previously designed in Dr. Moschou's lab, I chose a ratiometric analysis focusing on the alternative splicing effect of RBP1 and RBP1^{K55R}. Both proteins seemed to promote alternative splicing in a significantly different manner than negative control GV3011 (Figure 6D), while PTB3 and GRP7 were not found significantly altered. However, PTB3 has been previously found not to show major AS regulatory function compared to splicing factors PTB1 and PTB2.[118] GRP7 was reported to promote AS in response to RALF1-FERONIA complex activation, thereby the type of abiotic stress might not produce the same impact in AS.[105]

Immobilized Metal Affinity Chromatography (IMAC) using Ni beads lead to the purification of RBP1 and RBP1^{K55R} in large quantity and good levels of purity (Figure 6E). Purified protein is necessary for performing several *in vitro* phase separation. For example, contrast-based imaging methods, such as phase contrast and DIC that do not require extrinsic fluorophores could be performed, or quantitive approaches like FRAP (fluorescence recovery after photobleaching) and FLIP (fluorescence loss in photobleaching) to obtain quantitative information about the dynamics of fluorescently labeled components localized within phase-separated bodies.[128]

The RNA-binding domain of *N. tabacum* RBP1 has been characterized through NMR analysis before[107] (Figure 7A, top). *In silico* data support that RBP1 is a putative phase separating protein, at least driven by the IDR of the glycine-rich tail. Pi-pi interactions[30] show a high protein score of disorder for RBP1 phase separation (Figure 7A, middle left) and CIDER (Figure 7A,middle right), by calculating many different parameters associated with disordered protein sequences, places RBP1 close to Janus sequences, i.e collapsed or expanded sequences, where their behavior may depend on other factors (salt concentration, ligand binding, *cis*-interactions etc.).[121] Although PLDs and other disordered regions often display low sequence conservation, general sequence features, such as amino acid composition, are often conserved. [37,129] Adapting the same amino acid division into categories from Powers et al.[130], RBP1 shares a composition bias similar to prion-like proteins, showing similarity to PLD scaffolds that drive biomolecular condensate formation.

PONDR is a useful and long-established tool for disorder prediction.[122] By changing Tyrosines to Phenylalanines, a common substitution choice loss of phosphorylation, or else phospho-dead mutants, the disorder status of RBP1 is significantly changed from order to disorder (Figure 7B) in Y114F mutant, while Y129F shows the same disorder-to-order change and its impact is supported by a reported phosphorylation site in GRP7.[105] Transient expression of GFP- RBP1^{Y114F} and GFP-RBP1^{Y129F} in *N. benthamiana* showed same nuclear localization patterns in RT (Figure 7D, top). However, GFP- RBP1^{Y114F} formed more condensed ring-like structures and aggregate formation during heat stress, which could be related to the droplet-to-aggregate transition (Figure 7D, left column). GFP- RBP1^{Y129F} showed ring-like formations in RT and less nuclear puncta during heat stress (Figure 7D, right column). Overall, further studies following the same pipeline as K55R mutant (splicing probe, protein purification) are needed in order to elucidate the specific effects of these mutations to phase separation and function.

References

1. Friedman, J. R. & Nunnari, J. Mitochondrial form and function. *Nature* ***505***, 335–343 (2014).

2. Luzio, J. P., Pryor, P. R. & Bright, N. A. Lysosomes: fusion and function. *Nat Rev Mol Cell Biol* **8**, 622–632 (2007).

3. Hyman, A. A., Weber, C. A. & Jülicher, F. Liquid-Liquid Phase Separation in Biology. *Annu. Rev. Cell Dev. Biol.* **30**, 39–58 (2014).

4. Boeynaems, S. et al. Protein Phase Separation: A New Phase in Cell Biology. *Trends in Cell Biology* **28**, 420–435 (2018).

5. Shin, Y. & Brangwynne, C. P. Liquid phase condensation in cell physiology and disease. *Science* **357**, 4382 (2017).

6. Banani, S. F., Lee, H. O., Hyman, A. A. & Rosen, M. K. Biomolecular condensates: organizers of cellular biochemistry. *Nat Rev Mol Cell Biol* **18**, 285–298 (2017).

7. Mitrea, D. M. & Kriwacki, R. W. Phase separation in biology; functional organization of a higher order. *Cell Communication and Signaling* **14**, 1 (2016).

8. Monneron, A. & Bernhard, W. Fine structural organization of the interphase nucleus in some mammalian cells. *Journal of Ultrastructure Research* **27**, 266–288 (1969)

9. Brangwynne, C. P. *et al.* Germline P Granules Are Liquid Droplets That Localize by Controlled Dissolution/Condensation. *Science* **324**, 1729–1732 (2009)

10. Wang, J. *et al.* A Molecular Grammar Governing the Driving Forces for Phase Separation of Prion-like RNA Binding Proteins. *Cell* **174**, 688-699.e16 (2018).

11. Banani, S. F. et al. Compositional Control of Phase-Separated Cellular Bodies. *Cell* **166**, 651–663 (2016).

12. Hyman, A. A., Weber, C. A. & Jülicher, F. Liquid-Liquid Phase Separation in Biology. *Annu. Rev. Cell Dev. Biol.* **30**, 39–58 (2014).

13. Li, P. *et al.* Phase transitions in the assembly of multivalent signalling proteins. *Nature* **483**, 336–340 (2012).

14. Wheeler, J. R., Matheny, T., Jain, S., Abrisch, R. & Parker, R. Distinct stages in stress granule assembly and disassembly. *Elife* **5**, e18413 (2016).

15. Su, X. *et al.* Phase separation of signaling molecules promotes T cell receptor signal transduction. *Science* **352**, 595–599 (2016).

16. 16. Snead, W. T. & Gladfelter, A. S. The Control Centers of Biomolecular Phase Separation: How Membrane Surfaces, PTMs, and Active Processes Regulate Condensation. *Molecular Cell* **76**, 295–305 (2019).

17. Zhang, Y., Xu, B., Weiner, B. G., Meir, Y. & Wingreen, N. S. Decoding the physical principles of two-component biomolecular phase separation. *eLife* **10**, e62403 (2021).

18. Oldfield, C. J. & Dunker, A. K. Intrinsically Disordered Proteins and Intrinsically Disordered Protein Regions. *Annu. Rev. Biochem.* **83**, 553–584 (2014).

19. Oldfield, C. J. & Dunker, A. K. Intrinsically Disordered Proteins and Intrinsically Disordered Protein Regions. *Annu. Rev. Biochem.* **83**, 553–584 (2014).

20. van der Lee, R. *et al.* Classification of intrinsically disordered regions and proteins. *Chem Rev* **114**, 6589–6631 (2014).

21. Bah, A. & Forman-Kay, J. D. Modulation of Intrinsically Disordered Protein Function by Post-translational Modifications. *J Biol Chem* **291**, 6696–6705 (2016).

22. Wang, J., Shi, C., Xu, Q. & Yin, H. SARS-CoV-2 nucleocapsid protein undergoes liquid–liquid phase separation into stress granules through its N-terminal intrinsically disordered region. *Cell Discov* **7**, 1–5 (2021).

23. Chong, P. A., Vernon, R. M. & Forman-Kay, J. D. RGG/RG Motif Regions in RNA Binding and Phase Separation. *Journal of Molecular Biology* **430**, 4650–4665 (2018)..

24. Das, R. K., Ruff, K. M. & Pappu, R. V. Relating sequence encoded information to form and function of intrinsically disordered proteins. *Current Opinion in Structural Biology* **32**, 102–112 (2015).

25. Jensen, M. R., Ruigrok, R. W. & Blackledge, M. Describing intrinsically disordered proteins at atomic resolution by NMR. *Current Opinion in Structural Biology* **23**, 426–435 (2013).

26. Mittag, T. & Forman-Kay, J. D. Atomic-level characterization of disordered protein ensembles. *Current Opinion in Structural Biology* **17**, 3–14 (2007).

27. Thandapani, P., O'Connor, T. R., Bailey, T. L. & Richard, S. Defining the RGG/RG Motif. *Molecular Cell* **50**, 613–623 (2013).

28. Romero, P. *et al.* Sequence complexity of disordered protein. *Proteins: Structure, Function, and Bioinformatics* **42**, 38–48 (2001).

29. Phan, A. T. et al. Structure-function studies of FMRP RGG peptide recognition of an RNA duplex-quadruplex junction. *Nat Struct Mol Biol* **18**, 796–804 (2011)

30. Vernon, R. M. *et al.* Pi-Pi contacts are an overlooked protein feature relevant to phase separation. *eLife* **7**, e31486 (2018).

31. Frey, S., Richter, R. P. & Görlich, D. FG-rich repeats of nuclear pore proteins form a three-dimensional meshwork with hydrogel-like properties. *Science* **314**, 815–817 (2006).

32. Jain, S. et al. ATPase-Modulated Stress Granules Contain a Diverse Proteome and Substructure. *Cell* **164,** 487–498 (2016).

33. Kedersha, N. L., Gupta, M., Li, W., Miller, I. & Anderson, P. RNA-Binding Proteins Tia-1 and Tiar Link the Phosphorylation of Eif-2α to the Assembly of Mammalian Stress Granules. *Journal of Cell Biology* **147**, 1431–1442 (1999).

34. Chong, P. A., Vernon, R. M. & Forman-Kay, J. D. RGG/RG Motif Regions in RNA Binding and Phase Separation. *Journal of Molecular Biology* **430**, 4650–4665 (2018).

35. Boeynaems, S. *et al.* Phase Separation of C9orf72 Dipeptide Repeats Perturbs Stress Granule Dynamics. *Mol Cell* **65**, 1044-1055.e5 (2017).

36. Zarin, T. et al. Proteome-wide signatures of function in highly diverged intrinsically disordered regions. *eLife* **8**, e46883 (2019).

37. Zarin, T., Tsai, C. N., Nguyen Ba, A. N. & Moses, A. M. Selection maintains signaling function of a highly diverged intrinsically disordered region. *Proc Natl Acad Sci U S A* **114**, E1450–E1459 (2017).

38. Davey, N. E. The functional importance of structure in unstructured protein regions. *Current Opinion in Structural Biology* **56**, 155–163 (2019).

39. Davey, N. E. et al. Attributes of short linear motifs. Mol. *BioSyst.* **8,** 268–281 (2012).

40. Borgia, A. et al. Extreme disorder in an ultrahigh-affinity protein complex. *Nature* **555**, 61–66 (2018).

41. Fuxreiter, M. Fold or not to fold upon binding — does it really matter? *Current Opinion in Structural Biology* **54,** 19–25 (2019).

42. Wood, M. J., Storz, G. & Tjandra, N. Structural basis for redox regulation of Yap1 transcription factor localization. *Nature* **430**, 917–921 (2004).

43. del Rio, A. et al. Stretching Single Talin Rod Molecules Activates Vinculin Binding. *Science* **323**, 638–641 (2009).

44. Bah, A. *et al.* Folding of an intrinsically disordered protein by phosphorylation as a regulatory switch. *Nature* **519**, 106–109 (2015).

45. Petrey, D. & Honig, B. Structural Bioinformatics of the Interactome. *Annu. Rev. Biophys.* **43**, 193–210 (2014)

46. Neelamraju, Y., Hashemikhabir, S. & Janga, S. C. The human RBPome: from genes and proteins to human disease. *J Proteomics* **127**, 61–70 (2015).

47. Haynes, C. et al. Intrinsic Disorder Is a Common Feature of Hub Proteins from Four Eukaryotic Interactomes. *PLoS Comput Biol* **2**, e100 (2006).

48. Hubstenberger, A. *et al.* P-Body Purification Reveals the Condensation of Repressed mRNA Regulons. *Molecular Cell* **68**, (2017).

49. Youn, J.-Y. *et al.* Properties of Stress Granule and P-Body Proteomes. *Mol Cell* **76**, 286–294 (2019).

50. Brinegar, A. E. & Cooper, T. A. Roles for RNA-binding proteins in development and disease. *Brain Res* **1647**, 1–8 (2016).

51. Baralle, F. E. & Giudice, J. Alternative splicing as a regulator of development and tissue identity. *Nat Rev Mol Cell Biol* **18**, 437–451 (2017).

52. Marondedze, C. The increasing diversity and complexity of the RNA-binding protein repertoire in plants. *Proceedings of the Royal Society B: Biological Sciences* **287**, 20201397 (2020).

53. Wiedner, H. J. & Giudice, J. It's not just a phase: function and characteristics of RNA-binding proteins in phase separation. *Nat Struct Mol Biol* **28**, 465–473 (2021).

54. Riehs-Kearnan, N., Gloggnitzer, J., Dekrout, B., Jonak, C. & Riha, K. Aberrant growth and lethality of Arabidopsis deficient in nonsense-mediated RNA decay factors is caused by autoimmune-like response. *Nucleic Acids Research* **40**, 5615–5624 (2012).

55. Lou, L., Ding, L., Wang, T. & Xiang, Y. Emerging Roles of RNA-Binding Proteins in Seed Development and Performance. *International Journal of Molecular Sciences* **21**, 6822 (2020).

56. Lorković, Z. J. & Barta, A. Genome analysis: RNA recognition motif (RRM) and K homology (KH) domain RNA-binding proteins from the flowering plant Arabidopsis thaliana. *Nucleic Acids Res* **30**, 623–635 (2002).

57. Tam, P. P. C. *et al.* The Puf family of RNA-binding proteins in plants: phylogeny, structural modeling, activity and subcellular localization. *BMC Plant Biol* **10**, 44 (2010).

58. Owttrim, G. W. RNA helicases and abiotic stress. *Nucleic Acids Res* **34**, 3220–3230 (2006).

59. Sachetto-Martins, G., Franco, L. O. & de Oliveira, D. E. Plant glycine-rich proteins: a family or just proteins with a common motif? *Biochimica et Biophysica Acta (BBA) - Gene Structure and Expression* **1492**, 1–14 (2000).

60. Dreyfuss, G., Swanson, M. S. & Piñol-Roma, S. Heterogeneous nuclear ribonucleoprotein particles and the pathway of mRNA formation. *Trends in Biochemical Sciences* **13**, 86–91 (1988).

61. Maris, C., Dominguez, C. & Allain, F. H.-T. The RNA recognition motif, a plastic RNA-binding platform to regulate post-transcriptional gene expression. *The FEBS Journal* **272**, 2118–2131 (2005).

62. Adam, S. A., Nakagawa, T., Swanson, M. S., Woodruff, T. K. & Dreyfuss, G. mRNA polyadenylate-binding protein: gene isolation and sequencing and identification of a ribonucleoprotein consensus sequence. *Mol Cell Biol* **6**, 2932–2943 (1986).

63. Swanson, M. S., Nakagawa, T. Y., LeVan, K. & Dreyfuss, G. Primary structure of human nuclear ribonucleoprotein particle C proteins: conservation of sequence and domain structures in heterogeneous nuclear RNA, mRNA, and pre-rRNA-binding proteins. *Mol Cell Biol* **7**, 1731–1739 (1987).

64. Kenan, D. J., Query, C. C. & Keene, J. D. RNA recognition: towards identifying determinants of specificity. *Trends in Biochemical Sciences* **16**, 214–220 (1991).

65. Glisovic, T., Bachorik, J. L., Yong, J. & Dreyfuss, G. RNA-binding proteins and post-transcriptional gene regulation. *FEBS Lett* **582**, 1977–1986 (2008).

66. Ortega-Amaro, M. A. *et al.* Overexpression of AtGRDP2, a novel glycine-rich domain protein, accelerates plant growth and improves stress tolerance. *Frontiers in Plant Science* **5**, 782 (2015).

67. Gao, X. *et al.* A glycine-rich protein MoGrp1 functions as a novel splicing factor to regulate fungal virulence and growth in Magnaporthe oryzae. *Phytopathology Research* **1**, 2 (2019).

68. Condit, C. M. & Meagher, R. B. A gene encoding a novel glycine-rich structural protein of petunia. *Nature* **323**, 178–181 (1986).

69. Mangeon, A., Junqueira, R. M. & Sachetto-Martins, G. Functional diversity of the plant glycine-rich proteins superfamily. *Plant Signaling & Behavior* **5**, 99–104 (2010).

70. Fusaro, A. et al. Classification, expression pattern and comparative analysis of sugarcane expressed sequences tags (ESTs) encoding glycine-rich proteins (GRPs). *Genet. Mol. Biol.* **24**, 263–273 (2001).

71. Kupsch, C. et al. Arabidopsis Chloroplast RNA Binding Proteins CP31A and CP29A Associate with Large Transcript Pools and Confer Cold Stress Tolerance by Influencing Multiple Chloroplast RNA Processing Steps. *Plant Cell* **24**, 4266–4280 (2012).

72. Bocca, S. N. et al. Survey of glycine-rich proteins (GRPs) in the Eucalyptus expressed sequence tag database (ForEST). *Genet. Mol. Biol.* **28**, 608–624 (2005).

73. Li, Q. *et al.* Global Post-Translational Modification Discovery. *J. Proteome Res.* **16**, 1383–1390 (2017).

74. Owen, I. & Shewmaker, F. The Role of Post-Translational Modifications in the Phase Transitions of Intrinsically Disordered Proteins. *International Journal of Molecular Sciences* **20**, 5501 (2019).

75. Ryan, V. H. *et al.* Mechanistic View of hnRNPA2 Low-Complexity Domain Structure, Interactions, and Phase Separation Altered by Mutation and Arginine Methylation. *Mol Cell* **69**, 465-479.e7 (2018).

76. Qamar, S. et al. FUS Phase Separation Is Modulated by a Molecular Chaperone and Methylation of Arginine Cation-π Interactions. *Cell* **173**, 720-734.e15 (2018).

77. Ford, L., Ling, E., Kandel, E. R. & Fioriti, L. CPEB3 inhibits translation of mRNA targets by localizing them to P bodies. *PNAS* **116**, 18078–18087 (2019).

78. Zbinden, A., Pérez-Berlanga, M., De Rossi, P. & Polymenidou, M. Phase Separation and Neurodegenerative Diseases: A Disturbance in the Force. *Dev Cell* **55**, 45–68 (2020).

79. Keiten-Schmitz, J., Röder, L., Hornstein, E., Müller-McNicoll, M. & Müller, S. SUMO: Glue or Solvent for Phase-Separated Ribonucleoprotein Complexes and Molecular Condensates? *Front Mol Biosci* **8**, 673038 (2021).

80. Flotho, A. & Melchior, F. Sumoylation: A Regulatory Protein Modification in Health and Disease. *Annu. Rev. Biochem.* **82**, 357–385 (2013).

81. Rytz, T. C. et al. SUMOylome Profiling Reveals a Diverse Array of Nuclear Targets Modified by the SUMO Ligase SIZ1 during Heat Stress. *The Plant Cell* **30**, 1077–1099 (2018).

82. Conti, L. *et al.* Small ubiquitin-like modifier proteases OVERLY TOLERANT TO SALT1 and -2 regulate salt stress responses in Arabidopsis. *Plant Cell* **20**, 2894–2908 (2008).

83. Kurepa, J. *et al.* The Small Ubiquitin-like Modifier (SUMO) Protein Modification System in Arabidopsis: ACCUMULATION OF SUMO1 AND -2 CONJUGATES IS INCREASED BY STRESS*. *Journal of Biological Chemistry* **278**, 6862–6872 (2003).

84. Lee, J. *et al.* Salicylic acid-mediated innate immunity in Arabidopsis is regulated by SIZ1 SUMO E3 ligase. *Plant J* **49**, 79–90 (2007).

85. Murtas, G. *et al.* A nuclear protease required for flowering-time regulation in Arabidopsis reduces the abundance of SMALL UBIQUITIN-RELATED MODIFIER conjugates. *Plant Cell* **15**, 2308–2319 (2003).

86. Zhao, X. SUMO-Mediated Regulation of Nuclear Functions and Signaling Processes. *Molecular Cell* **71**, 409–418 (2018).

87. Lin, X.-L. *et al.* An Arabidopsis SUMO E3 Ligase, SIZ1, Negatively Regulates Photomorphogenesis by Promoting COP1 Activity. *PLOS Genetics* **12**, e1006016 (2016).

88. Yates, G., Srivastava, A. K. & Sadanandom, A. SUMO proteases: uncovering the roles of deSUMOylation in plants. *Journal of Experimental Botany* **67**, 2541–2548 (2016).

89. Komander, D. & Rape, M. The Ubiquitin Code. *Annu. Rev. Biochem.* **81**, 203–229 (2012).

90. Corpet, A. *et al.* PML nuclear bodies and chromatin dynamics: catch me if you can! *Nucleic Acids Research* **48**, 11890–11912 (2020).

91. Lallemand-Breitenbach, V. & de Thé, H. PML nuclear bodies: from architecture to function. *Current Opinion in Cell Biology* **52**, 154–161 (2018).

92. Morita, Y., Kanei-Ishii, C., Nomura, T. & Ishii, S. TRAF7 Sequesters c-Myb to the Cytoplasm by Stimulating Its Sumoylation. *MBoC* **16**, 5433–5444 (2005).

93. Plaschka, C., Lin, P.-C., Charenton, C. & Nagai, K. Prespliceosome structure provides insights into spliceosome assembly and regulation. *Nature* **559**, 419–422 (2018).

94. Syed, N. H., Kalyna, M., Marquez, Y., Barta, A. & Brown, J. W. S. Alternative splicing in plants – coming of age. *Trends in Plant Science* **17**, 616–623 (2012).

95. mRNA Processing and Metabolism. *Methods and Protocols*. (2004).

96. Hendriks, I. A. & Vertegaal, A. C. O. A comprehensive compilation of SUMO proteomics. *Nat Rev Mol Cell Biol* **17**, 581–595 (2016)

97. Zhou, J., Zhao, S. & Dunker, A. K. Intrinsically Disordered Proteins Link Alternative Splicing and Post-translational Modifications to Complex Cell Signaling and Regulation. *Journal of Molecular Biology* **430**, 2342–2359 (2018).

98. Staiger, D., Zecca, L., Kirk, D. A. W., Apel, K. & Eckstein, L. The circadian clock regulated RNA-binding protein AtGRP7 autoregulates its expression by influencing alternative splicing of its own pre-mRNA. *The Plant Journal* **33**, 361–371 (2003).

99. Heintzen, C., Nater, M., Apel, K. & Staiger, D. AtGRP7, a nuclear RNA-binding protein as a component of a circadian-regulated negative feedback loop in Arabidopsis thaliana. *PNAS* **94**, 8515–8520 (1997).

100. Carpenter, C. D., Kreps, J. A. & Simon, A. E. Genes Encoding Glycine-Rich Arabidopsis thaliana Proteins with RNA-Binding Motifs Are Influenced by Cold Treatment and an Endogenous Circadian Rhythm. *Plant Physiology* **104**, 1015–1025 (1994).

101. Kwak, K. J., Kim, Y. O. & Kang, H. Characterization of transgenic Arabidopsis plants overexpressing GR-RBP4 under high salinity, dehydration, or cold stress. *J Exp Bot* **56**, 3007–3016 (2005).

102. Cao, S., Jiang, L., Song, S., Jing, R. & Xu, G. AtGRP7 is involved in the regulation of abscisic acid and stress responses in arabidopsis. *Cellular and Molecular Biology Letters* **11**, 526–535 (2006).

103. Fu, Z. Q. et al. A type III effector ADP-ribosylates RNA-binding proteins and quells plant immunity. *Nature* **447**, 284–288 (2007).

104. Heintzen, C. *et al.* A light- and temperature-entrained circadian clock controls expression of transcripts encoding nuclear proteins with homology to RNA-binding proteins in meristematic tissue. *The Plant Journal* **5**, 799–813 (1994).

105. Wang, L. *et al.* RALF1-FERONIA complex affects splicing dynamics to modulate stress responses and growth in plants. *Science Advances* **6**, eaaz1622.

106. Haruta, M., Sabat, G., Stecker, K., Minkoff, B. B. & Sussman, M. R. A Peptide Hormone and Its Receptor Protein Kinase Regulate Plant Cell Expansion. *Science* **343**, 408–411 (2014).

107. Khan, F. *et al.* Structural basis of nucleic acid binding by Nicotiana tabacum glycine-rich RNA-binding protein: implications for its RNA chaperone function. *Nucleic Acids Res* **42**, 8705–8718 (2014).

108. Bot, P., Khan, F., Sultana, T., Deeba, F. & Naqvi, S. M. S. DYNAMICS OF mRNA OF GLYCINE-RICH RNA-BINDING PROTEIN DURING WOUNDING, COLD AND SALT STRESSES IN NICOTIANA TABACUM. *Pakistan Journal of Botany* **45**, 297–300 (2013).

109. Jabeen, B. *et al.* Ectopic Expression of Plant RNA Chaperone Offering Multiple Stress Tolerance in E. coli. *Mol Biotechnol* **59**, 66–72 (2017).

110. Ziemienowicz, A., Haasen, D., Staiger, D. & Merkle, T. Arabidopsis transportin1 is the nuclear import receptor for the circadian clock-regulated RNA-binding protein AtGRP7. *Plant Mol Biol* **53**, 201–212 (2003).

111. Karapidaki, I. «Ρόλος της πρωτεΐνης RNA Binding Protein 1 σε φυτά Nicotiana tabacum υπό συνθήκες αβιοτικής καταπόνησης». (University of Crete, 2021).

112. Madeira, F. *et al.* The EMBL-EBI search and sequence analysis tools APIs in 2019. *Nucleic Acids Res* **47**, W636–W641 (2019).

113. Chang, C.-C., Tung, C.-H., Chen, C.-W., Tu, C.-H. & Chu, Y.-W. SUMOgo: Prediction of sumoylation sites on lysines by motif screening models and the effects of various post-translational modifications. *Sci Rep* **8**, 15512 (2018).

114. Bi, H. *et al.* SUMOylation of GPS2 protein regulates its transcription-suppressing function. *MBoC* **25**, 2499–2508 (2014).

115. Kang, F. *et al.* E-syt1 Re-arranges STIM1 Clusters to Stabilize Ring-shaped ER-PM Contact Sites and Accelerate Ca2+ Store Replenishment. *Sci Rep* **9**, 3975 (2019).

116. Kim, J. S. *et al.* Glycine-rich RNA-binding protein 7 affects abiotic stress responses by regulating stomata opening and closing in Arabidopsis thaliana. *Plant J* **55**, 455–466 (2008).

117. Stefano, G. *et al.* In tobacco leaf epidermal cells, the integrity of protein export from the endoplasmic reticulum and of ER export sites depends on active COPI machinery. *The Plant Journal* **46**, 95–110 (2006).

118. Rühl, C. *et al.* Polypyrimidine Tract Binding Protein Homologs from Arabidopsis Are Key Regulators of Alternative Splicing with Implications in Fundamental Developmental Processes[W]. *Plant Cell* **24**, 4360–4375 (2012).

119. Di Gioacchino, M., Ricci, M. A., Imberti, S., Holzmann, N. & Bruni, F. Hydration and aggregation of a simple amino acid: The case of glycine. *Journal of Molecular Liquids* **301**, 112407 (2020).

120. Sherrill, C. D. Energy Component Analysis of π Interactions. *Acc. Chem. Res.* **46**, 1020–1028 (2013)..

121. Holehouse, A. S., Ahad, J., Das, R. K. & Pappu, R. V. CIDER: Classification of Intrinsically Disordered Ensemble Regions. *Biophysical Journal* **108**, 228a (2015).

122. Garner, null, Romero, null, Dunker, null, Brown, null & Obradovic, null. Predicting Binding Regions within Disordered Proteins. *Genome Inform Ser Workshop Genome Inform* **10**, 41–50 (1999).

123. Wen, J. *et al.* Conformational Expansion of Tau in Condensates Promotes Irreversible Aggregation. *J. Am. Chem. Soc.* **143**, 13056–13064 (2021).

124. Zhu, J.-K. Abiotic stress signaling and responses in plants. *Cell* **167**, 313–324 (2016).

125. Zhu, J.-K. Abiotic stress signaling and responses in plants. *Cell* **167**, 313–324 (2016).

126. Takeno, K. Stress-induced flowering: the third category of flowering response. *Journal of Experimental Botany* **67**, 4925–4934 (2016).

127. Knight, H., Trewavas, A. J. & Knight, M. R. Cold calcium signaling in Arabidopsis involves two cellular pools and a change in calcium signature after acclimation. *Plant Cell* **8**, 489–503 (1996).

128. Mitrea, D. M. *et al.* Methods for Physical Characterization of Phase-Separated Bodies and Membrane-less Organelles. *Journal of Molecular Biology* **430**, 4773–4805 (2018).

129. Riback, J. A. et al. Stress-Triggered Phase Separation Is an Adaptive, Evolutionarily Tuned Response. *Cell* **168**, 1028-1040.e19 (2017).

130. Powers, S. K. *et al.* Nucleo-cytoplasmic Partitioning of ARF Proteins Controls Auxin Responses in Arabidopsis thaliana. *Molecular Cell* **76**, 177-190.e5 (2019).

Chapter II. Unraveling the role of Kin7.3 in blue light signaling

Introduction

Introduction -Chapter II

KISC -it's complicated

Cell polarity, vaguely defined as the establishment of asymmetry inside the cell, is a necessary feature of cell function and is tightly linked to developmental and environmental regulation, growth, and morphogenesis.[131] *Radially swollen4* (rsw4) is a temperature-sensitive point mutant of the EXTRA SPINDLE POLE (ESP) gene encoding the caspase-related protease separase[132] that presents disorganized cortical microtubules, which in turn disrupt cell morphology and polarity.[133] Recent work in Dr. Moschou's lab showed that separase affects membrane protein trafficking and the polar targeting of the auxin efflux carrier PIN-FORMED2 (PIN2) to the rootward side of the root cortex cells.[134] To achieve this function in cell polarity, *Arabidopsis thaliana* ESP (AtESP) interacts *in vitro* and *in vivo* with a previously uncharacterized class of microtubule motors that belong to a CENP-E-related clade of kinesins (Kin7.3 clade), thereby forming the KInesin Separase Complex; KISC[135] that promotes microtubule stability (Figure 1). Yet, the role of Kin7.3 in other developmental processes beyond root development remains largely unknown.

AtESP and Kin7.3 -the on/off switch

By performing a yeast two-hybrid (Y2H) screen of a universal Arabidopsis library using N-terminal, central, and C-terminal fragments of AtESP as baits, Moschou et al.[135] discovered the C-terminal region of a putative microtubule-based motor (AT3G12020.1) as an interactor of the N-terminal domain of AtESP. Designated as Kinesin 7.3, the interactor belongs to group 7 (Kin7) of the kinesin superfamily and, in absence of AtESP, Kin7.3 appears to function in an auto-inhibitory manner. Conformational changes induced by the folding of the C-terminal tail to the N-terminal motor domain block the interaction of Kin7.3 with microtubules, while AtESP abolishes this auto-inhibitory effect by interacting with the tail domain of Kin7.3 (Figure 1A). Thus, the N-terminal motor becomes available for interaction with microtubules (Figure 1A). Kin7.3 belongs to a clade of five *Arabidopsis* proteins together with Kin7.1 (AT1G21730), Kin7.2 (AT2G21380), Kin7.4 (AT4G39050), and Kin7.5 (AT5G06670). Additionally, it was shown that AtESP does not only interact with Kin7.3, but also with Kin7.1 and Kin7.5, suggesting functional redundancy in KISC functions.[135]

Kinesins -it's all about class

Kinesins comprise a superfamily of ATP-driven microtubule-based motor enzymes that gain the necessary energy for mechanical work onto microtubule tracks by hydrolyzing ATP.[136] Kinesin motor proteins have been reported to be involved in the local positioning of organelles and molecules, through the facilitation of short-distance movements along microtubules.[137] Kinesin motor proteins are found in all eukaryotic organisms[138], classified into ~17 families based on the phylogenetic analysis of their motor domains. Kinesin-1 to kinesin-14 have been long established as protein families[139], kinesin-15 to kinesin-17 were recently identified and some kinesin proteins remain ungrouped, without a distinct phylogenetic classification. Despite the identification of 61

different kinesin-encoding genes with high motor domain similarity in *Arabidopsis thaliana*[140], the remaining non-motor sequences do not share common features.[141] In plants, kinesins have been reportedly involved in various cellular activities, regulating the orientation of deposition of cellulose myofibrils[142], interacting with a geminivirus replication protein[143], morphogenesis [144,145], mitosis, and meiosis. [146–152] Surprisingly, the kinesin-7 and 14 families account for more than half of the kinesins encoded by the Arabidopsis genome. This abundance, specifically in plants, suggests the evolution of specified functions, such as flower morphogenesis, trichome development, cell division, and phragmoplast formation [151,153] or the substitution of the functions of animal motors absent in plants, like animal dyneins, by the motors of kinesin-14 family.[141]

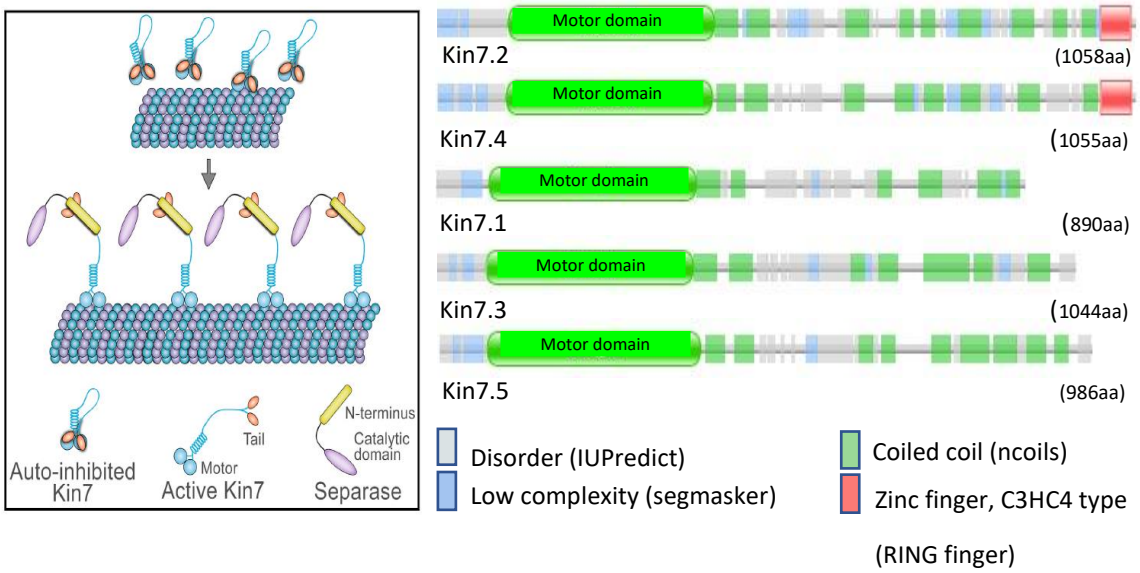

Figure 2. (A) Schematic representation of KISC binding onto microtubules. Reprinted from Moschou et al.[6] (B) Overview of the Kin 7 family, protein domains and predicted disorder regions by Pfam, based on UNIPROT.aa; amino acids.

Microtubules -the (cyto)skeletons in the closet

Microtubules are dynamic polymers of αβ-tubulin heterodimers, regulated by the hydrolysis of β-tubulin-bound GTP after a tubulin dimer has been incorporated into the microtubule end, albeit with a delay.[154] The newly formed microtubule tip contains a cap of GTP-tubulin (denoted the GTP cap), featuring stabilizing properties, whereas the microtubule shaft is composed of GDP-tubulin and is defined as intrinsically unstable.[155] Dynamic instability, a microtubule behavior by which MTs within a population coexist and interconvert in states of growth and shrinkage[156], is much more dynamic in cells instead of pure MT solutions, supporting the existence of cellular factors that regulate dynamics. [157] Microtubule-associated proteins (MAPs) interact with the microtubule end, including microtubule polymerases, microtubule depolymerases, and regulatory kinesins, acting cooperatively and competitively to determine whether the microtubule grows or shrinks.[158–160] Plant microtubules form dense and organized arrays called cortical microtubules (CMTs) at the periphery of the cell during interphase, mainly to guide the trajectory of the

transmembrane cellulose synthase complex.[161] In response to light, plants use mechanisms to switch the orientation of their cortical microtubule array, and therefore the morphology and function of the cells that harbor them[162,163] (Figure 2A, B). In rapidly elongating cells of the embryonic shoot axis (a tissue known as the hypocotyl), where CMTs are organized transversely to the axis of cell and tissue growth, blue light (BL) stimulation triggers a 90° microtubule array reorientation within minutes[164–166], redirecting cellulose deposition to build and organize the cell wall. Microtubule nucleation and severing machineries are orchestrated in microtubule reorientation through phototropin (BL receptors, see below) activities in response to BL.[167] For this reason, microtubule BL-induced reorientation is significantly decreased in etiolated (grown in darkness) hypocotyl cells in *phototropin* and *katanin*(microtubule severing protein) mutants (Figure 2B,C).[168]

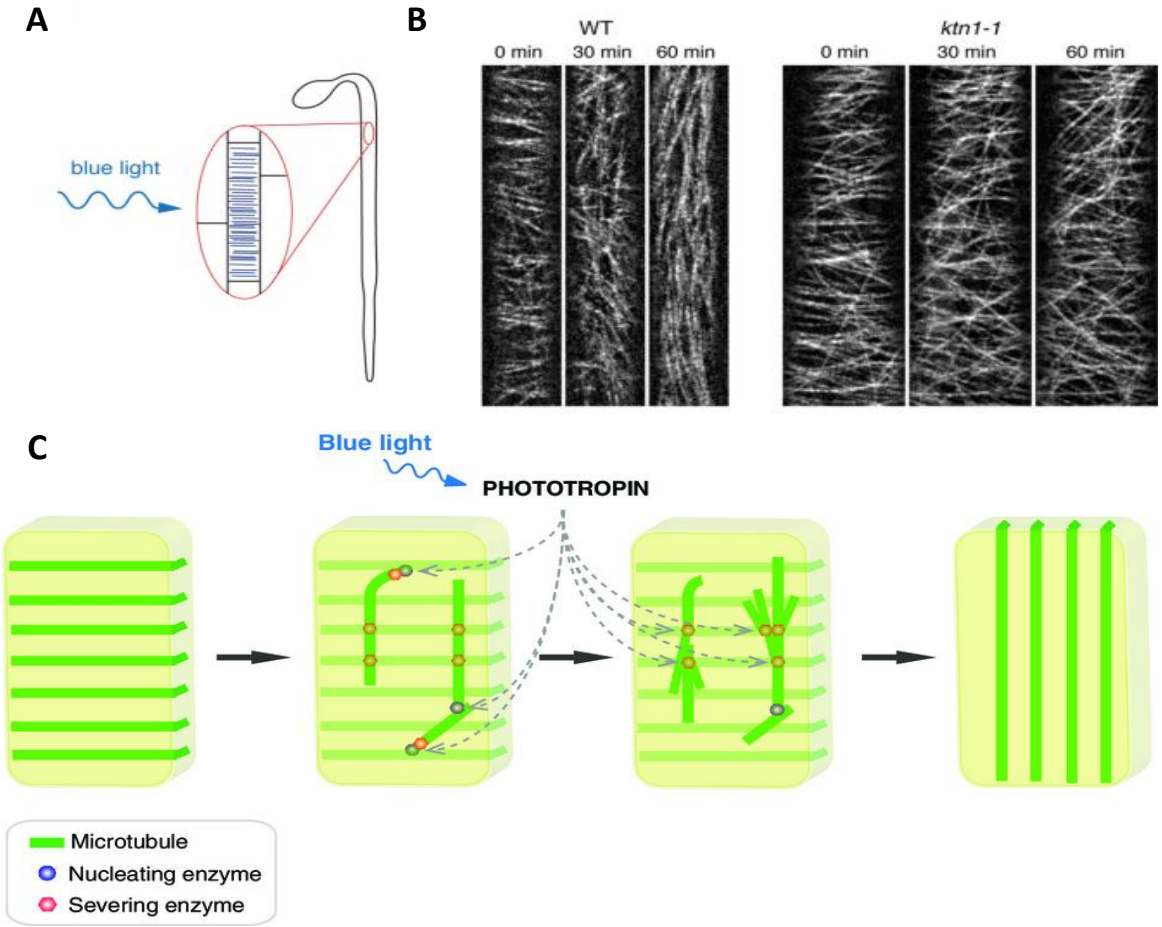

Figure 3. (A) Schematic drawing indicates location of imaging and angular coordinates for experiment in B, (B)Microtubule reorientation induced by blue light in WT and ktn1-1 mutants, expressing mCherry-TUA5 (tubulin-a chain), (C) A model for CMT reorientation in response to blue light irradiation and mediated by phototropins, where crossovers of longitudinal microtubules with preexisting transverse arrays are sites of localization and activation of severing enzymes. (A) and (B) adapted by Lindeboom et al.[41] and (C) reprinted by Nakamura.[42]

Phototropism -go into the light

Phototropism, the differential cell elongation responding to directional BL, offers photosynthetic light capture optimization to plants, with specific photoreceptors and signaling pathways orchestrating light adaptation.[169] These components integrate signals of light quality and quantity, to adaptively modify overall growth characteristics from seed germination to reproduction.[170–172] Phototropism is specifically induced by UV-A/BL and can be divided into two phases, depending on the fluence and time requirements.[173] First-positive curvature is generally described as the bending of shoots toward unilateral BL by brief pulses at very low fluences, while second-positive curvature occurs with prolonged irradiation in a time-dependent manner.[174] Plant phototropism is predominantly controlled by blue-light photoreceptors, the phototropins, known principally for their key role in phototropism response and characterized as blue (390–500 nm) and ultraviolet-A (320–390 nm) photoreceptors.[175] PHOT1 acts as the dominant receptor, mediating response across a wide range of fluence rates (e.g. 0.01–100 µmol m^{-2} s^{-1}), whereas PHOT2 appears to operate only at higher fluence rates (>10 µmol m^{-2} s^{-1}).[176] Higher plants share two different phototropins, namely PHOT1 and PHOT2, with gene duplication events discovered in some species' genome.[177] PHOT1 and PHOT2 regulate many physiological activities beside the regulation of hypocotyl and root phototropism[176] and seem to be functionally redundant for chloroplast accumulation movement[178], stomatal opening[179,180], leaf positioning and leaf flattening**.**

Phototropins -feeling the blues

Structurally, the phototropins consist of two major regions, an amino-terminal photosensory domain and a carboxyl-terminal Ser/Thr protein kinase signaling domain (Figure 3). The photosensory domain consists of two ∼110 amino acid homologous islands, critical for photoreceptor activity called LOV1 (light, oxygen, voltage) and LOV2[181], which function as binding sites for the BL-absorbing chromophore flavin mononucleotide (FMN). The LOV1 domain is primarily responsible for phototropin di/multimerization [54–56], while LOV2 mainly regulates the C-terminal kinase domain through a BL-induced derepression.[186–189] In the dark, LOV2 binds to the kinase domain and inhibits its phosphorylation activity.[190] Upon photoexcitation, the binding of LOV2 to the kinase domain is inhibited, resulting in the activation of kinase activity and receptor autophosphorylation.[163,191,192] An α–helix (designated Jα) associates with the surface of LOV2 in the dark state and is disrupted upon cysteinyl adduct formation by photoactivation of FMN. Thus, Jα-helix turns into a disordered state, with site-directed mutagenesis studies showing that the unfolding of the Jα-helix results in activation of the C-terminal kinase domain.[183,193]

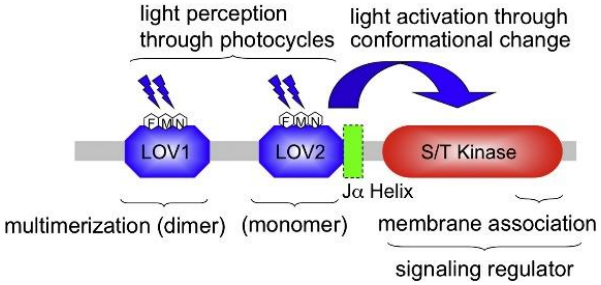

Figure 4. Schematic illustration of structural, functional and regulatory properties of phototropins. Photocycles of LOV domains result in conformational changes in LOV2-Ja helix association, consequently leading to downstream signaling by kinase domain activation. The C-terminus plays a key role in membrane association of phototropins. Reprinted by Kong, S-.M. and Wada, M. [57]

Phototropins and light signaling -don't shoot the messenger

BL excitation induces intermolecular interactions between PHOT1 molecules in the plasma membrane (MB) and leads to autophosphorylation, which results in an increased dimerization rate and an immediate, but partial internalization of the photoreceptor into the cytoplasm[162,194], whereas PHOT2 reportedly associates with the Golgi apparatus.[195,196] The first step of BL signaling activation involves the dimerization of PHOT1 and its relocalization at sterol-rich membrane microdomains (MM) of the PM (Figure 4A), observed through FRET (Förster or fluorescence resonance energy transfer) analysis with the PM microdomain marker AtREM1.3.[194] Following activation, phototropins are internalized to inner compartments and show mosaic-like formations (Figure 4B), possibly through clathrin-mediated endocytosis.[197] It was shown that CULLIN3-based E3 ubiquitin ligase, $CRL3^{NPH3}$ marks PHOT1 through mono/multiubiquitination and affects phototropism.[198] Recent work showed that SUMOylation, a similar process to ubiquitination, is also implicated in phototropin responses.[199] Autophosphorylation of PHOT1 in the activation loop appears as a prerequisite for PHOT1 activation and PHOT1-mediated responses, with Ser-851 and Ser-849 being important phosphorylation sites.[192] Yet, another study showed that modifications that can anchor PHOT1 receptor to the PM, such as myristoylation or farnesylation, diminish the light-induced internalization of PHOT1, without impacting functions such as phototropism or chloroplast accumulation movement.[200]

NPH3 and light signaling –when a third person comes in between

Unilateral irradiation results in phototropic curvature (Figure 2A), orchestrated by the establishment of a photoreceptor activation gradient between the irradiated and the shaded

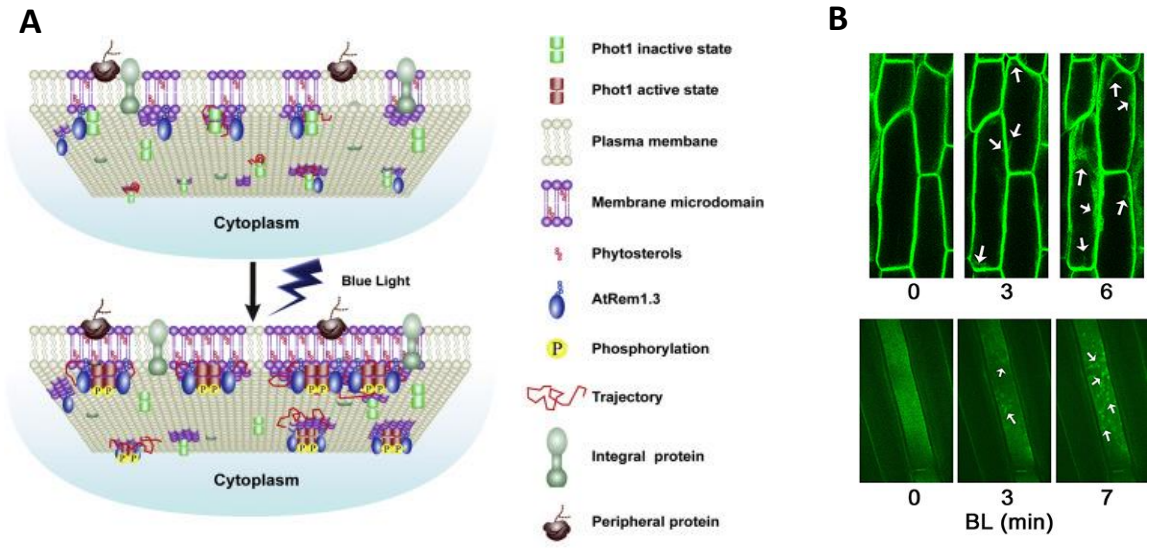

Figure 5.(A) Proposed model for microdomain organization of PHOT1 activation under blue light irradiation. After BL exposure, activated PHOT1 sequentially undergoes dimerization and phosphorylation, with phosphorylation increasing PHOT1 self-association in MMs and AtRem1.3 (marker of sterol-rich lipid environments). Reprinted by Xue et al.[71] (B) (upper) Blue light-induced mobility of PHOT1-GFP from the plasma membrane to the cytoplasm in etiolated hypocotyl cells of Arabidopsis, (lower) spinning disc confocal microscopy of cortical cells in elongation zone, showing punctuate aggregation and mosaic formation after blue light irradiation. Reprinted by Liscum.[76]

side.[201,202] In the darkness, the signal NONPHOTOROPIC HYPOCOTYL 3 (NPH3) resides in a phosphorylated state and localizes to the PM, interacting with the N-terminal portion of PHOT1 through its C-terminal region. [203–205] After PHOT1 BLactivation and autophosphorylation, NPH3 is de-phosphorylated in a PHOT1-dependent and darkness-reversible manner and becomes internalized into aggregates, a process that transiently attenuates its interaction with PHOT1.[205,206] Phosphorylation of NPH3 is necessary for the formation of an active signaling complex with PHOT1 at the PM[207], supported by recent data demonstrating that the phosphorylation status of NPH3 does not affect the expression or autophosphorylation activity of PHOT1. Rather, NPH3 maintains the balance between the active and steady states of PHOT1 signaling and contributes to the robustness of hypocotyl phototropism across a broad range of blue-light intensities.[208] NPH3 is also part of the CULLIN3 RING E3 UBIQUITIN LIGASE complex that ubiquitinates PHOT1, as aforementioned. [198,209] NPH3 is an essential component of light signaling and phototropic curvature, a process combined with the formation of the lateral gradient of auxin.[210]

Auxin and PINs –nothing can PIN me down

Auxin is a key hormone in basically all differentiation processes throughout plant development, responsible also for tropic responses, such as phototropic curvature.[211] Phototropic curvature is accomplished by auxin transport, achieved by a system of auxin influx and efflux transporters.[212] Efflux carrier PIN-FORMED (PIN) proteins are reportedly involved in the modulation of auxin flow and establishment of auxin gradient.[169,213] The contributions of *PIN1*, *PIN3*, and *PIN7* gene mutants to phototropic hypocotyl bending in short BLpulse excitation are obvious compared to defects by long-term BLtreatment, such as those employed in most phototropism studies.[214,215] During phototropic bending of the hypocotyl, the polarity of PIN3 protein changes upon light exposure from apolar to greatly decreased in the outer lateral side of endodermal cells, a polarity switch necessary for auxin redistribution in the hypocotyl and efficient phototropism. [213,216] Both the *trans*-hypocotyl gradient of auxin and PIN3 polarity can be completely negated in a *phot1* mutant background.[216] Hence, auxin gradients facilitate the phototropic response by establishing the curvature formation. A rather complex relationship between KISC, light-signaling modules, the cytoskeleton, and auxin distribution is plotted by combining the aforementioned information, pointing to the necessity of examining the details of their association.

Aim of study -Chapter II

My thesis aimed to investigate the role of Kin7.3 in light signaling. This work was built on preliminary results from Dr. Moschou's lab, suggesting that Kin7.3 interacts with PHOT1. Yet, the role and function of Kin7.3 in BL response remained uncharacterized. Therefore, I followed:

(i) a genetic approach to examine whether and how Kin7.3 affects PHOT1-dependent response to BL

(ii) a cell biology approach to investigate whether Kin7.3 affects PHOT1 localization patterns and microtubule reorganization

Results -Chapter II

Previous work in Dr. Moschou's lab established the role of Kin7.3 in regulating auxin signaling and cell polarity.[135] To discover additional roles of Kin7.3 in plant signaling, the interactome of Kin7.3 by mass spectrometry after affinity purification was performed in collaboration with the lab of Dr. Yasin Dagdas (GMI, Austria). Semi-comparative analysis of the identified peptides in the GFP-Kin7.3 sample compared to the GFP control indicated the light-signaling protein PHOT1 as a promising Kin7.3 interactor (Figure 5A). These results revealed an unknown interplay between Kin7.3 and light-signaling responses, albeit in need of further experimental validation, due to the regular false-positive results.[217,218]

Since the motor domain of kinesins associates with microtubules, the truncated version of the tail domain of Kin7.3 (KIN7.3T) was employed in previous experiments of Fragkiadaki[219] as a possible interaction domain. Transient expression of Kin7.3 fused to YFP and under 35S ubiquitous promoter (35S:YFP-Kin7.3) and PHOT1 inserted into pTAP vector (TAP includes 9XMYC-6xHIS-3C cleavage site-2xIgG binding domain) under 35S ubiquitous promoter (35S:PHOT1-TAP) was performed. Subsequently, samples were treated with blue and white light before collection and utilized for Co-IP experiments using GFP-trap beads. Results from Fragkiadaki[219] confirmed that GFP-Kin7.3 interacted *in vivo* with PHOT1-TAP in both white light (150 µmol m^{-2} s^{-1}) conditions, under which PHOT1 was active and with Far-Red (FR) light (25 µmol m^{-2} s^{-1}) conditions, under which PHOT1 was inactive (Figure 5 B). No interaction was observed between PHOT1-TAP and free GFP (eGFP), which was used as negative control. Aside from the *in vivo* confirmation of interaction, the implications of different light properties in Kin7.3 association with PHOT1 are beyond the scope of this study.

PHOT1 acts as a key receptor in phototropic responses[175], raising the question of whether Kin7.3 affects phototropism through this interaction. To test the role of Kin7.3 in the phototropic response, a genetic approach was selected for the investigation of the effect of Kin7.3 loss of function in hypocotyl curvature, in response to directional BL. For this experiment, the previously described *k135* triple mutant, a triple knock-out of Kin7.1, Kin7.3, and Kin7.5, was selected due to Kin7.1,3 and 5 playing redundant roles in plant development.[135] The *k135* mutant harbors T-DNA insertion, either in the motor or the tail domain of Kinesins, and the presence of the insertion was validated through genotyping (Supplemental Figures, 2A). In further detail, etiolated seedlings of Arabidopsis lines Col-0, *k135, phot1-5, phot 2-1,* and *nph3* were exposed to directional low intensity BL (0.1 µmol m^{-2} s^{-1}). As expected according to relevant literature, while wild-type (WT) Col-0 seedlings bent towards the direction of the light source (curvature), the insensitive *phot1-5* (PHOT1 BL receptor loss-of-function mutant) served as a negative control. PHOT1 signaling during curvature response is also dependent on interaction with NPH3[207], in agreement with *nph3* lines showing insensitivity to BL-induced curvature. In accordance with previous studies that showed PHOT2 not affecting phototropism in low-BL[194,220,221], *phot2-1* mutant presented positive phototropism.[169,206,213,222] My results showed that *k135* was irresponsive to phototropism compared to the Col-0, and to a lesser extent than the *phot1-5* and *nph3* mutants (Figure 5C).

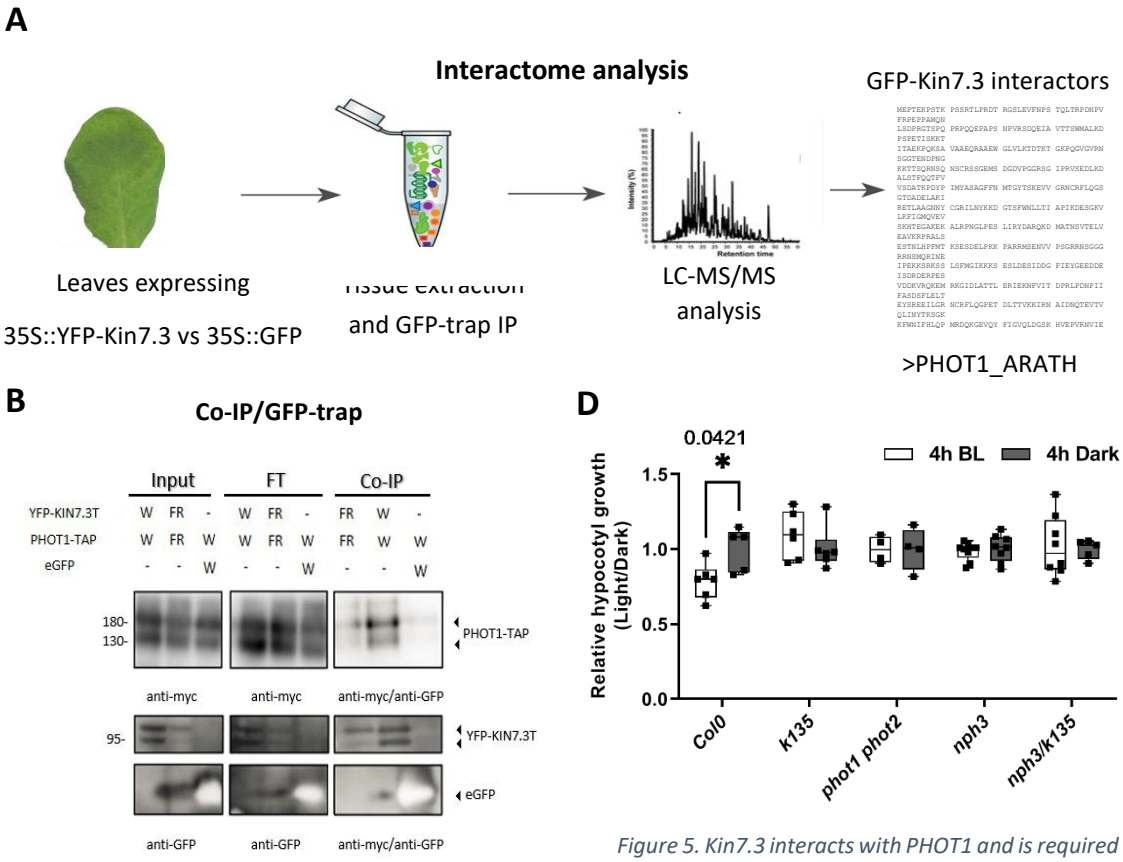

Figure 5. Kin7.3 interacts with PHOT1 and is required for blue light-induced responses. (A) Experimental pipeline for the in vivo discovery approach of Kin7.3 interactomeby MS. Unpublished data from Dr. Moschou's lab, (B) Co-immunoprecipitation of transiently expressed in N.benthamiana PHOT1-TAP with YFP-Kin7.3t. Membrane was probed with anti-myc, stripped and re-probed with anti-GFP (IP). Figure adapted from Fragkiadaki[89], (C) Quantification of hypocotyl curvature experiment. Graphs show deviation of Col-0, k135, nph3, phot1-5 and phot2-1 from the vertical axis. Statistical analysis was performed using Krustal-Wallis non parametric test and Dunnets post hoc test. Experimental design was followed as in Christie et al.[87], (D) Relative hypocotyl growth inhibition of etiolated Col-0, k135, phot1 phot2, nph3 and nph3/k135. Statistical analysis of growth in the Dark versus light was performed using two-way ANOVA, $p<0.05$.

Further confirmation of the importance of Kin7.3 in phototropic response was explored by performing BL-induced hypocotyl inhibition experiments. The hypocotyl growth of seedlings was measured after an 4h exposure to continuous BL (1 µmol m^{-2} s^{-1}), with attention not to disturb the controlled BL conditions inside the dark chamber that BL experiments were conducted. After

treatment, I calculated the relative inhibition of hypocotyl growth, by comparing growth in BL versus darkness-grown seedlings. For instance, it is known that Arabidopsis *phot1-5* mutants do not show rapid BL induced inhibition of hypocotyl growth.[223] Preliminary results showed that, while Col-0 seedlings presented a significant difference in hypocotyl growth inhibition following BL treatment, the *k135* mutant was insensitive to the BL and continued grow. Intriguingly, although NPH3 is reportedly not necessary for phototropin-mediated growth inhibition[223], in this experiment we also observed insensitivity to the BL-induced inhibition for the *nph3* mutant (Figure 5D).

PHOT1 acts as a PM-associated receptor, and studies in PHOT2 suggested that PM anchoring is probably established through a short stretch of amino acids in the C-terminal region of the protein.[224] Studies have shown that activation of PHOT1-GFP by BL triggers a dynamic reorganization of PHOT1-GFP in the PM and intracellular compartments. Initially, PHOT1-GFP presents a mostly homogenous distribution at the PM, with BL stimulation resulting in a reorganization of PHOT1 PM localization patterns to a more "patchy" distribution, probably representing clusters or microdomains.[225] A few minutes after the photoreaction, PHOT1-GFP starts to internalize to intracellular compartments.[197] Despite the possible interference of the C-terminal GFP tag to the short stretch of PHOT1 C-terminal amino acids, cell fractionation studies have confirmed that BL-induced native and GFP-tagged PHOT1 internalize from the PM to cytosolic locations.[226] Due to the importance of the relocalization of PHOT1-GFP in PM microdomains or its internalization for signaling and phototropic responsiveness, I aimed to compare the localization dynamics of PHOT1-GFP in WT with PHOT1-GFP in *k135* background.

At the start of this master thesis, transgenic lines expressing PHOT1-GFP lines under the regulatory regions of endogenous promoters were available (a gift from Prof. John Christie), as also the first progeny of PHOT1-GFP cross with Kin7.3 mutant. To confirm the appropriate background for BL experiments, the PHOT1-GFP/*k135* lines were validated through genotyping and selved (Supplemental Figures, 2A) until homozygosity was achieved. Detailed analysis of PHOT1-GFP localization was performed by confocal imaging, with the help and guidance of Dr. Moschou in the performing time course analysis through confocal imaging. Four day old dark-grown seedlings were treated with BL and observed through a time-course analysis assay. In good agreement with previous studies, it was evident that dark-grown PHOT1-GFP in Col-0 background was initially relatively evenly distributed at the PM (Figure 6A, t_{0min}). However, a few minutes later it formed rapidly distinct mosaics with strongly labeled punctate areas[225] (Figure 6A, t_{4min}) and at the end, it obtained polarized distribution at the PM (Figure 6A, t_{8min}). Interestingly, by investigating PHOT1-GFP in *k135* background localization, I observed that PHOT1-GFP expression was higher and possibly resulted in increased PM localization. We found that PHOT1-GFP was still internalized in the *k135*, but this internalization might had been delayed in the *k135* mutant background. However, these data are preliminary. Following experiments will soon involve the investigation of PHOT1-GFP mobility at the PM in WT and *k135* background by FRAP (Fluorescence recovery after photobleaching) and also to measure turnover PHOT1 rate at the PM in the WT and *k135* background.

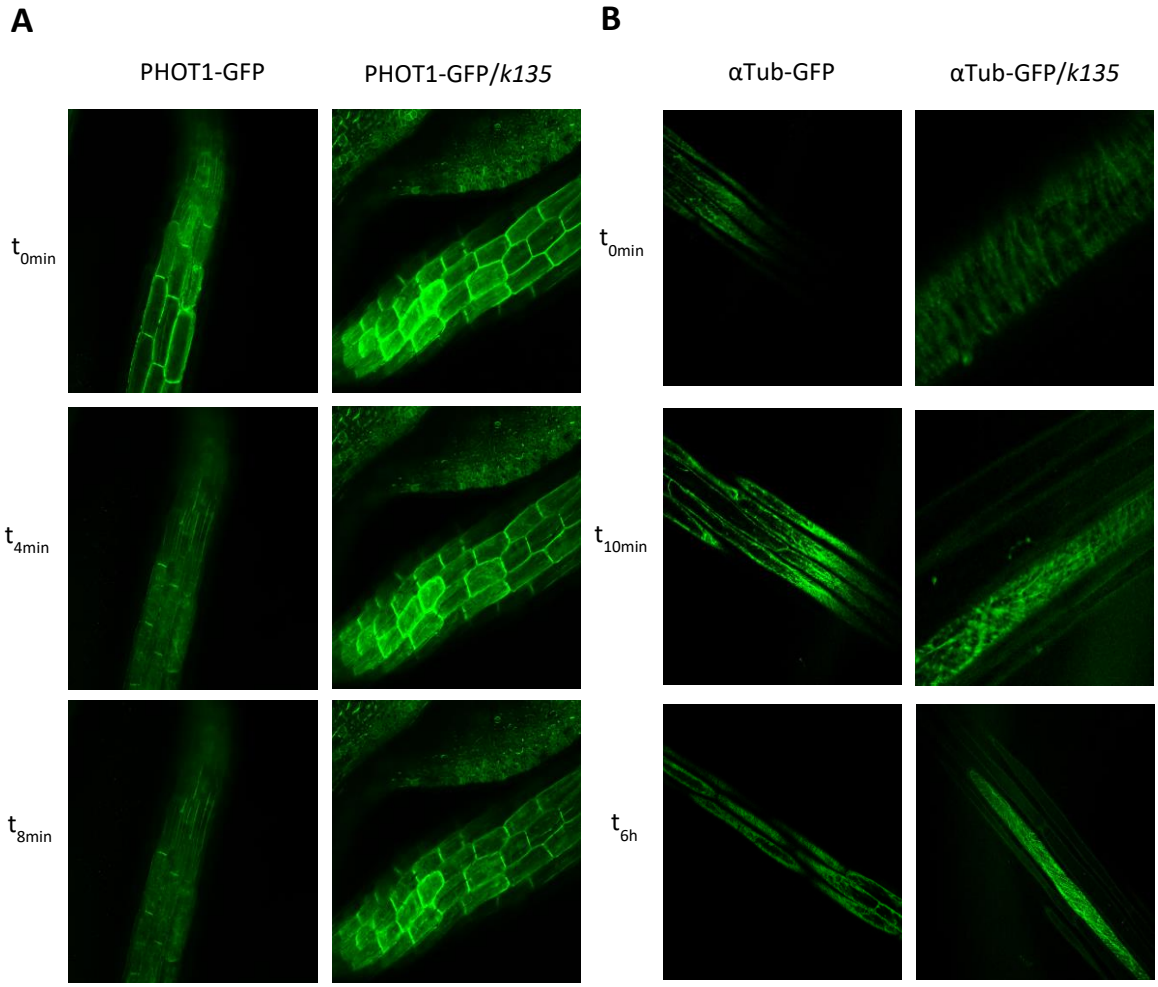

Figure 6. Kin7.3 affects localization of Phot1-GFP, changes localization and affects microtubule reorganization upon BL treatment. (A)Time-course analysis of hypocotyl epidermal cells expressing 35S:PHOT1-GFP in Col-0 and k135 background, respectively, showing increased expression of 35S:PHOT1-GFP in k135 lines. Confocal images were captured at t_{0min}, t_{4min} and t_{8min}, after exposure to continuous BL, (B) Time-course analysis of hypocotyl epidermal cells expressing αTubulin-GFP in Col-0 and k135 background, respectively. Microtubule reorganization (t_{0min}) recovery to transverse arrays (t_{10min}) is altered in k135 (t_{6h}).

Yet, there are controversial reports about whether receptor internalization is necessary for phototropism[200]. Kin7.3 associates with microtubules and, since microtubule organization is important for microdomain signaling platform formation[194], it is possible that Kin7.3 regulates the phototropic responsiveness through regulation of the PHOT1-GFP signaling complexes at the PM. Further experiments using super resolution microscopy should be performed, to confirm this hypothesis.

Due to previous works using drug treatments[227] or *katanin*[168] mutants[192] suggesting that cytoskeleton and microtubules are important elements in phototropic response, I investigated whether Kin7.3 alters microtubule organization. When dark-grown *A.thaliana* seedlings are

irradiated with blue light, microtubules arrays reorient from transverse to longitudinal. Transverse microtubules are ultimately replaced with longitudinal ones, due to the increase of microtubule severing activity induced by BL.[168,228] Thus, I validated through genotyping transgenic lines of α-tubulin fused C-terminally with GFP expressed under a ubiquitous 35S promoter (αTub-GFP) in Col-0 and *k135* background and examined them by confocal imaging. Figure 6B shows the immediate reorganization of microtubule arrays from transverse (Figure 6B, t_{0min}) to longitudinal (Figure 6B, t_{10min}) in both WT and *k135* lines, as previously described for Col-0 lines.[168] However, after 6h of continuous BL treatment, α-Tub-GFP line showed rearrangement of microtubule arrays from longitudinal to transverse in Col-0, whereas *k135* features microtubules resistant to initial array reorganization(Figure 6B, t_{6h}). αTub-GFP shows that, while *k135* responds to BL by the rapid microtubule reorganization and facilitates phototropic responses, it might also face long-term effects impacting cytoskeleton properties.

PHOT1 reportedly exhibits reduced electrophoretic mobility after blue-light irradiation *in vivo*, consistent with the kinase activity that leads to the autophosphorylation of the receptor.[229] PHOT1-GFP, under the control of the native PHOT1 promoter, has been shown to complement the null *phot1-5* allele[230] and exhibits a similar reduction in electrophoretic mobility from darkness to BL treatment, even after 5 min of exposure to BL.[192,229] Using these observations, I investigated the effect of *k135* in PHOT1-GFP activation by examining its electrophoretic mobility by Western Blot, using anti-GFP antibodies. My results showed that PHOT1-GFP BL-induced band shift was reduced in the *k135* mutant background, yet with less electrophoretic mobility difference than in the *nph3* background (Figure 7A). These results suggest that Kin7.3 might affect the levels of autophosphorylation of PHOT1 and thus its activation at the PM, which could explain the phototropic response insensitivity of the *k135* line in BL treatment.

Kinesins are often modified by phosphorylation and this phosphorylation can affect its conformation states and interactions [192] and Kin7.3 is reportedly phosphorylated in multiple serine and theronine sites.[231] Indeed, mass spectrometry analysis of GFP-Kin7.3 also identified several phosphorylation sites (unpublished data, Dr. Moschou's lab). I identified GFP-Kin7.3 *in vivo* phosphorylation sites by searching public databases (Arabidopsis Protein Phosphorylation Site Database, PhosPhAt 4.0[231]), combined them with phosphorylation sites identified by mass spectrometry in the Kin7.3 interactome study (Figure 7B), and designed primers to perform single site or combinatory Kin7.3 point mutant to alanine (loss of phosphorylation, or phospho-dead mutants) for future functional and localization assays. I also investigated the conservation of these phosphorylation sites, by performing alignment of Kin7.1, Kin7.3, and Kin7.5 using ClustalW[112] (Figure 7,B). During my work, I generated three Kin7.3 point phosphorylation mutants in entry clones (pZEO, Supplemental Figures, 2B) that will be exploited in future work in the lab.

A

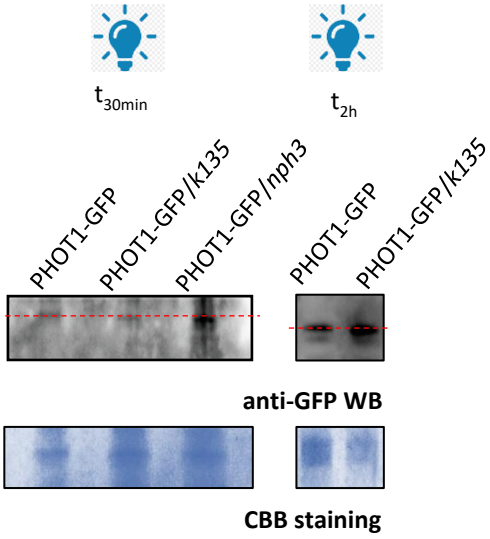

Figure 7. PHOT1 phosphorylation status may be dependent on Kin7.3. (A) Western blot of PHOT1-GFP, PHOT1-GFP/k135 and PHOT1-GFP/nph3 lines. The molecular weight band swift of PHOT1-GFP is reduced in k135 and nph3 background and suggests that Kin7.3 plays a role in PHOT1 BL-induced phosphorylation or activation. Membrane was probed with anti-GFP and stained with CBB: Coomassie Blue staining, (B) Kin7.1, Kin7.2 and Kin7.3 alignment and conservation analysis by ClustalW and phosphorylation site prediction by PhosPhAt 4.0.[231] Tail; start of tail region, blue color; conserved aminoacids, green color; phosphorylated aminoacids based on public phosphorylation database research and by MS in Dr.Moschou's lab, orange colour: identified only by other studies.

B

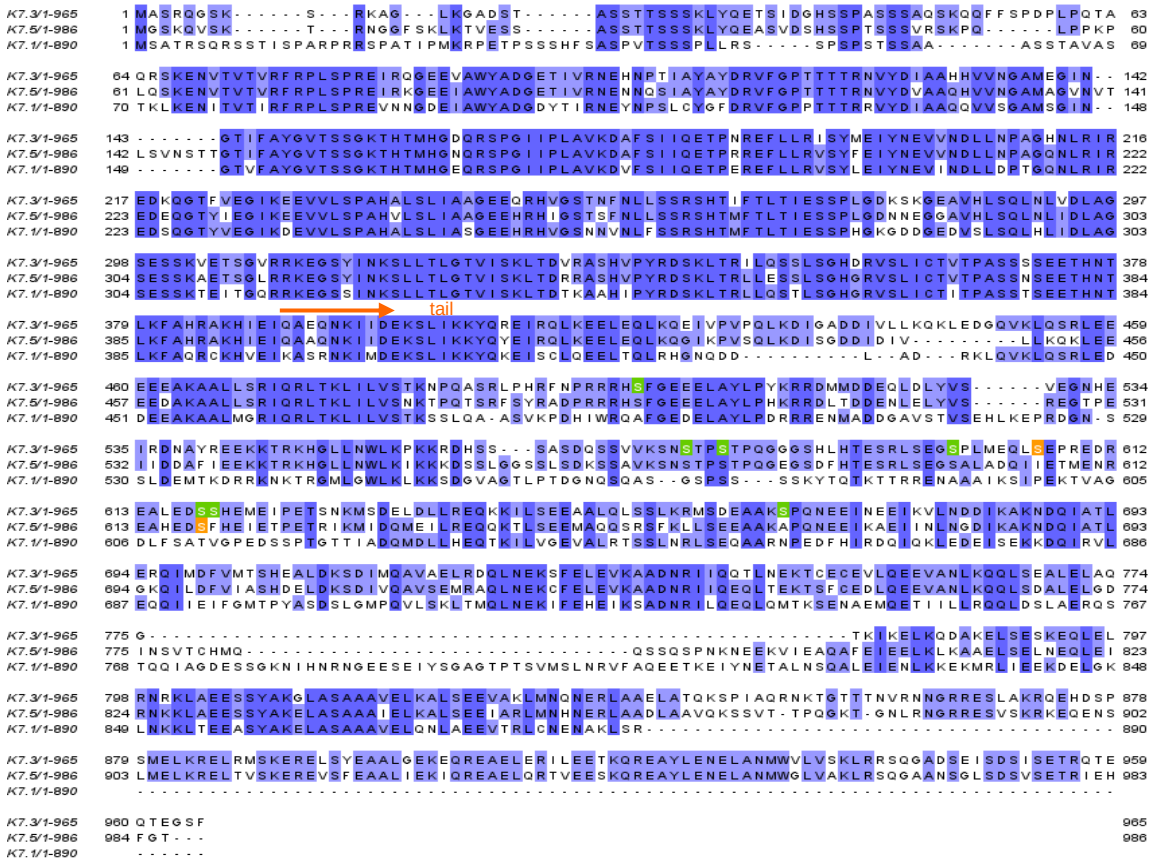

Discussion -Chapter II

BL photoreceptors are key components of a core signaling hub[232], controlling the growth of plants to the most optimal position for survival and growth. Light-emitting diode (LED) lights with a wide range of customized light spectra are used to grow plants in vertical farms, highlighting the importance of understanding the inner workings of BL response. Deciphering the intricate workings of BL signaling pathways is a topic of study that has been extensively explored in the past and Kin7.3 seems to be implicated in multiple functions, especially in so far unexplored BL signaling pathways. Mass spectrometry results (Figure 5A) from Dr. Moschou's lab have placed Kin7.3 as a possible interactor of PHOT1 and Fragkiadaki [219] has shown in vitro proof of PHOT1-Kin7.3 interaction (Figure 5B) in BL treatments, further supporting their association. Transgenic lines of *k135* based on the redundant roles of Kin7.1,3 and 5[135] have displayed insensitivity to key phototropic responses, such as BL-induced bending (curvature, Figure 5C). Collectively, these functional assays indicate that Kin7.3 is a novel component of the PHOT1-dependent signaling.

Extensive studies of PHOT1 function and localization have elucidated several details of the signaling events that are triggered by PHOT1 activation due to BL, raising the question of how Kin7.3 might be implicated in these phenomena. My major observations based on localization studies involve (i) GFP-PHOT1 showing increased expression levels when expressed in the *k135* mutant background and (ii) GFP-PHOT1 presenting a more pronounced and slightly delayed dissociation from the PM (Figure 6B). One hypothesis might be that PHOT1-GFP turnover and degradation are altered in the *k135* mutant background and that the lack of Kin7.3 is responsible for these increased levels. Another hypothesis could link the difference in signal intensity to enhanced self-association of PHOT1 in PM in *k135* at the levels of the PM, which is known to occur immediately after BL treatment.[194] The delay of GFP-PHOT1 dissociation from the PM could be caused by the reduced activation of PHOT1 in the PM, following BL treatment and subsequent internalization. For example, the lack of Kin7.1,3 or 5 could have a direct effect on microtubules (or indirect, i.e. by promoting the expression of other kinesins), which could have an impact on the composition and/or properties of the BL-induced PHOT1-associated microdomains. Indeed, current knowledge on microdomain formation suggests that the cytoskeleton acts as fences that transiently confine membrane proteins and organize signaling platforms.[233] In terms of cytoskeletal effects of Kin7.3 in BL stimulated responses, αTub-GFP showed resistance in microtubule reversion to their previous array organization (Figure 6B). One explanation could be possible microtubule nucleation deficiencies caused by the lack of Kin7.3, despite previous findings suggesting this role for Kin14 and Kin5, but not the Kin7 family.[234]

The electrophoretic shift of PHOT1 in the *k135* background suggests that PHOT1 is not phosphorylated in the same manner as PHOT1 in the Col-0 background (Figure 7A). This band 'shift' could be related to functional implications of *k135* background, suggesting that Kin7.3 might be involved in some step of PHOT1 phosphorylation. NPH3 is necessary for BL signaling activation[207] and the phosphorylation status of PHOT1 appeared, at least, partially inflicted by the

lack of this signaling complex partner. However, to confirm the phosphorylation levels of PHOT1 and further evaluate whether Kin7.3 is actively participating in the signaling pathway, phospho-antibodies should be used in Western blot analysis by following the same pipeline to support this claim.

According to PhosphAt 4.0 database, Kin7.3 is phosphorylated in multiple serine/threonine sites (Figure 7B). Post-translational modifications, such as phosphorylation, might affect protein conformation by changing the protein's structural properties, stability, and dynamics[235] that could, in turn, play a significant role in Kin7.3-PHOT1 interaction. Mass spectrometry results (unpublished data from Dr. Moschou's lab) have also identified phosphorylated Serines in Kin7.3, adding to the importance of deciphering its role, even out of the scope of BL induced responses.

Since PHOT1 forms complexes with multiple partners that affect signaling activity, it would be interesting to investigate the role of Kin7.3 in the context of these interactions. As mentioned earlier, auxin gradients are a major contributor to achieving phototropism. [211] Efflux auxin carrier PIN proteins have been extensively studied for their effect in BL-induced responses.[211] Genetic crosses between GFP-fused PIN proteins and *k135* are in progress, to determine whether Kin7.3 is involved in establishing auxin gradients or, possibly, by disturbing microtubule reorganization and auxin deposition. This is particularly relevant, as previous work in the lab showed that Kin7.3 plays a role in the regulation of cell polarity and auxin signaling in the roots.[135]

Future experiments will involve a more extensive study of PHOT1-Kin7.3 interaction, by BIFC (BImolecular Fluorescent Complementation). BIFC is a visualization technique for protein-protein interaction, based on the reconstitution of e.g. YFP halves fused to two proteins that interact intracellularly.[236] Also, MG132 treatment, which effectively blocks the proteolytic activity of the 26S proteasome complex[237], could provide some insight into the internalization and degradation of PHOT1 in parallel with the lack of Kin7.3 expression. Lastly, advanced microscopy techniques such as FRAP (Fluorescence recovery after photobleaching) and TIRF (Total Internal Reflection Fluorescence) could aid in measuring or estimating the dynamic movement of PHOT1 in PM and how this is affected in the *k135* background.

References

131. Yang, Z. Cell polarity signaling in Arabidopsis. *Annu Rev Cell Dev Biol*. **24**, 551-575 (2008).

132. Wiedemeier A. *et al*. Mutant alleles of *Arabidopsis RADIALLY SWOLLEN 4* and *7* reduce growth anisotropy without altering the transverse orientation of cortical microtubules or cellulose microfibrils. *Development* **129**, 4821–4830 (2002.)

133. Wu, S. *et al.* A conditional mutation in Arabidopsis thaliana separase induces chromosome non-disjunction, aberrant morphogenesis and cyclin B1;1 stability. *Development* **137**, 953–961 (2010).

134. Moschou, P. N. *et al.* The Caspase-Related Protease Separase (EXTRA SPINDLE POLES) Regulates Cell Polarity and Cytokinesis in Arabidopsis. *The Plant Cell* **25**, 2171–2186 (2013).

135. Moschou, P. N., Gutierrez-Beltran, E., Bozhkov, P. V. & Smertenko, A. Separase Promotes Microtubule Polymerization by Activating CENP-E-Related Kinesin Kin7. *Developmental Cell* **37**, 350–361 (2016).

136. Ali, I. & Yang, W.-C. Why are ATP-driven microtubule minus-end directed motors critical to plants? An overview of plant multifunctional kinesins. *Functional Plant Biol.* **47**, 524 (2020).

137. Cai, G. & Cresti, M. Microtubule motors and pollen tube growth--still an open question. *Protoplasma* **247**, 131–143 (2010).

138. Wickstead, B., Gull, K. Richards TA. Patterns of kinesin evolution reveal a complex ancestral eukaryote with a multifunctional cytoskeleton. *BMC Evol Biol*. **10**, 1471-2148 (2010).

139. Lawrence, C. J. *et al*. A standardized kinesin nomenclature. *J Cell Biol*. **167**, (1):19-22 (2004).

140. Reddy, A. S. & Day, I. S. Kinesins in the Arabidopsis genome: a comparative analysis among eukaryotes. *BMC Genomics* **2**, 2 (2001).

141. Ali, I. & Yang, W.-C. The functions of kinesin and kinesin-related proteins in eukaryotes. *Cell Adh Migr* **14**, 139–152.

142. Zhong, R., Burk, D.H., Morrison, W.H. 3rd, Ye, Z.H. A kinesin-like protein is essential for oriented deposition of cellulose microfibrils and cell wall strength. *Plant Cell*. **14**, (12):3101-3117.(2002).

143. Kong, L.J., Hanley-Bowdoin, L. A geminivirus replication protein interacts with a protein kinase and a motor protein that display different expression patterns during plant development and infection. *Plant Cell.* **14,** (8):1817-32. (2002).

144. Ambrose, J. C., Li, W., Marcus, A., Ma, H. & Cyr, R. A Minus-End–directed Kinesin with Plus-End Tracking Protein Activity Is Involved in Spindle Morphogenesis. *MBoC* **16**, 1584–1592 (2005).

145. Higgins, D. M., Nannas, N. J. & Dawe, R. K. The Maize Divergent spindle-1 (dv1) Gene Encodes a Kinesin-14A Motor Protein Required for Meiotic Spindle Pole Organization. *Frontiers in Plant Science* **7**, 1277 (2016).

146. Liu, B., Cyr, R. J. & Palevitz, B. A. A kinesin-like protein, KatAp, in the cells of arabidopsis and other plants. *The Plant Cell* **8**, 119–132 (1996).

147. Lee, Y.-R. J., Giang, H. M. & Liu, B. A Novel Plant Kinesin-Related Protein Specifically Associates with the Phragmoplast Organelles. *The Plant Cell* **13**, 2427–2439 (2001).

148. Lee, Y.-R. J., Li, Y. & Liu, B. Two Arabidopsis Phragmoplast-Associated Kinesins Play a Critical Role in Cytokinesis during Male Gametogenesis. *The Plant Cell* **19**, 2595–2605 (2007).

149. Chen, C. *et al.* The Arabidopsis ATK1 gene is required for spindle morphogenesis in male meiosis. *Development* **129**, 2401–2409 (2002).

150. Nishihama, R. *et al*. Expansion of the Cell Plate in Plant Cytokinesis Requires a Kinesin-like Protein/MAPKKK Complex. *Cell* **109**, 87–99 (2002).

151. Ambrose, J. C. & Cyr, R. Mitotic Spindle Organization by the Preprophase Band. *Molecular Plant* **1**, 950–960 (2008).

152. Wordeman, L., How kinesin motor proteins drive mitotic spindle function: Lessons from molecular assays. *Seminars in Cell & Developmental Biology*, **21,** (3):.260-268 (2010).

153. Asada, T., Kuriyama, R. & Shibaoka, H. TKRP125, a kinesin-related protein involved in the centrosome-independent organization of the cytokinetic apparatus in tobacco BY-2 cells. *J Cell Sci* **110 (Pt 2)**, 179–189 (1997).

154. Ravelli, R. B. G. *et al.* Insight into tubulin regulation from a complex with colchicine and a stathmin-like domain. *Nature* **428**, 198–202 (2004).

155. Hunter, A. & Wordeman, L. How motor proteins influence microtubule polymerization dynamics. *Journal of Cell Science* **113**, 4379-4389 (2000).

156. Mitchison, T. & Kirschner, M. Dynamic instability of microtubule growth. *Nature* **312**, 237–242 (1984).

157. Walczak, C. E., Gayek, S. & Ohi, R. Microtubule-Depolymerizing Kinesins. *Annu. Rev. Cell Dev. Biol.* **29**, 417–441 (2013).

158. Akhmanova, A. & Steinmetz, M. Tracking the ends: a dynamic protein network controls the fate of microtubule tips. *Nature Reviews Molecular Cell Biology* **9**, 309-322 (2008)

159. Akhmanova, A. & Steinmetz, M. O. Control of microtubule organization and dynamics: two ends in the limelight. *Nat Rev Mol Cell Biol* **16**, 711–726 (2015).

160. Howard, J. & Hyman, A. A. Microtubule polymerases and depolymerases. Current Opinion in Cell Biology 19, 31–35 (2007).

161. Ledbetter, M. C. & Porter, K. R. A 'MICROTUBULE' IN PLANT CELL FINE STRUCTURE. *Journal of Cell Biology* **19**, 239–250 (1963).

162. Roll-Mecak, A. Shining Light at Microtubule Crossroads. *Science* **342**, 1180–1181 (2013).

163. Inoue, S., Kinoshita, T., Takemiya, A., Doi, M. & Shimazaki, K. Leaf positioning of Arabidopsis in response to blue light. *Mol Plant* **1**, 15–26 (2008).

164. Laskowski, MartaJ. Microtubule orientation in pea stem cells: a change in orientation follows the initiation of growth rate decline. *Planta* **181**, (1990).

165. Ueda, K. & Matsuyama, T. Rearrangement of cortical microtubules from transverse to oblique or longitudinal in living cells of transgenicArabidopsis thaliana. *Protoplasma* **213**, 28–38 (2000).

166. Nick, P., Bergfeld, R., Schäfer, E. & Schopfer, P. Unilateral reorientation of microtubules at the outer epidermal wall during photo- and gravitropic curvature of maize coleoptiles and sunflower hypocotyls. *Planta* **181**, 162–168 (1990).

167. Nakamura, M. Microtubule nucleating and severing enzymes for modifying microtubule array organization and cell morphogenesis in response to environmental cues. *New Phytologist* **205**, 1022–1027 (2015).

168. Lindeboom, J. J. *et al.* A mechanism for reorientation of cortical microtubule arrays driven by microtubule severing. *Science* **342**, 1245533 (2013).

169. Liscum, E. *et al.* Phototropism: Growing towards an Understanding of Plant Movement. *The Plant Cell* **26**, 38–55 (2014).

170. Kami, C., Lorrain, S., Hornitschek, P. & Fankhauser, C. Chapter Two - Light-Regulated Plant Growth and Development. in *Current Topics in Developmental Biology* **91,** 29–66 (2010).

171. Pedmale, U. V., Celaya, R. B. & Liscum, E. Phototropism: Mechanism and Outcomes. *Arabidopsis Book* **8**, e0125 (2010).

172. Chen, M. & Chory, J. Phytochrome signaling mechanisms and the control of plant development. *Trends in Cell Biology* **21**, 664–671 (2011).

173. Iino, M. Chapter 23 Phototropism in higher plants. *Comprehensive Series in Photosciences* **1**, 659–811 (2001)

174. Iino, M. Toward understanding the ecological functions of tropisms: interactions among and effects of light on tropisms. *Current Opinion in Plant Biology* **9,** 89–93 (2006)

175. Briggs, W. R. & Christie, J. M. Phototropins 1 and 2: versatile plant blue-light receptors. *Trends in Plant Science* **7**, 204–210 (2002).

176. Sakai, T. et al. Arabidopsis nph1 and npl1: Blue light receptors that mediate both phototropism and chloroplast relocation. *Proceedings of the National Academy of Sciences* **98**, 6969–6974 (2001).

177. Li, F.-W. *et al.* The origin and evolution of phototropins. *Front. Plant Sci.* **6**, (2015).

178. Kagawa, T. Arabidopsis NPL1: A Phototropin Homolog Controlling the Chloroplast High-Light Avoidance Response. *Science* **291**, 2138–2141 (2001).

179. Kinoshita, T. et al. phot1 and phot2 mediate blue light regulation of stomatal opening. *Nature* **414**, 656–660 (2001).

180. Inoue, S., Takemiya, A. & Shimazaki, K. Phototropin signaling and stomatal opening as a model case. *Curr Opin Plant Biol* **13**, 587–593 (2010).

181. Christie, J. M. Phototropin Blue-Light Receptors. *Annu. Rev. Plant Biol.* **58**, 21–45 (2007).

182. Salomon, M., Lempert, U. & Rüdiger, W. Dimerization of the plant photoreceptor phototropin is probably mediated by the LOV1 domain. *FEBS Letters* **572**, 8–10 (2004).

183. Nakasako, M., Zikihara, K., Matsuoka, D., Katsura, H. & Tokutomi, S. Structural Basis of the LOV1 Dimerization of Arabidopsis Phototropins 1 and 2. *Journal of Molecular Biology* **381**, 718–733 (2008).

184. Nakasone, Y., Zikihara, K., Tokutomi, S. & Terazima, M. Photochemistry of Arabidopsis phototropin 1 LOV1: transient tetramerization. *Photochem Photobiol Sci* **12**, 1171–1179 (2013).

185. Kong, S.-G. & Wada, M. Recent advances in understanding the molecular mechanism of chloroplast photorelocation movement. *Biochimica et Biophysica Acta (BBA) - Bioenergetics* **1837**, 522–530 (2014).

186. Christie, J. M., Swartz, T. E., Bogomolni, R. A. & Briggs, W. R. Phototropin LOV domains exhibit distinct roles in regulating photoreceptor function. *The Plant Journal* **32,** 205–219 (2002).

187. Okajima, K., Kashojiya, S. & Tokutomi, S. Photosensitivity of Kinase Activation by Blue Light Involves the Lifetime of a Cysteinyl-Flavin Adduct Intermediate, S390, in the Photoreaction Cycle of the LOV2 Domain in Phototropin, a Plant Blue Light Receptor *. *Journal of Biological Chemistry* **287**, 40972–40981 (2012).

188. Tokutomi, S., Matsuoka, D. & Zikihara, K. Molecular structure and regulation of phototropin kinase by blue light. *Biochimica et Biophysica Acta (BBA) - Proteins and Proteomics* **1784**, 133–142 (2008).

189. Wang, J. *et al.* Phototropin 1 Mediates High-Intensity Blue Light-Induced Chloroplast Accumulation Response in a Root Phototropism 2-Dependent Manner in Arabidopsis phot2 Mutant Plants. *Frontiers in Plant Science* **12**, 2044 (2021).

190. Christie, J. M., Salomon, M., Nozue, K., Wada, M. & Briggs, W. R. LOV (light, oxygen, or voltage) domains of the blue-light photoreceptor phototropin (nph1): Binding sites for the chromophore flavin mononucleotide. *PNAS* **96**, 8779–8783 (1999).

191. Salomon, M., Christie, J. M., Knieb, E., Lempert, U. & Briggs, W. R. Photochemical and mutational analysis of the FMN-binding domains of the plant blue light receptor, phototropin. *Biochemistry* **39**, 9401–9410 (2000).

192. Sullivan, S., Thomson, C. E., Lamont, D. J., Jones, M. A. & Christie, J. M. In vivo phosphorylation site mapping and functional characterization of Arabidopsis phototropin 1. *Mol Plant* **1**, 178–194 (2008).

193. Harper, S. M., Christie, J. M. & Gardner, K. H. Disruption of the LOV-Jalpha helix interaction activates phototropin kinase activity. *Biochemistry* **43**, 16184–16192 (2004).

194. Xue, Y. *et al.* Arabidopsis Blue Light Receptor Phototropin 1 Undergoes Blue Light-Induced Activation in Membrane Microdomains. *Molecular Plant* **11**, 846–859 (2018).

195. Aggarwal, C. *et al.* Blue-light-activated phototropin2 trafficking from the cytoplasm to Golgi/post-Golgi vesicles. *J Exp Bot* **65**, 3263–3276 (2014).

196. Kong, S.-G. *et al.* Blue light-induced association of phototropin 2 with the Golgi apparatus. *The Plant Journal* **45**, 994–1005 (2006).

197. Kaiserli, E., Sullivan, S., Jones, M. A., Feeney, K. A. & Christie, J. M. Domain Swapping to Assess the Mechanistic Basis of Arabidopsis Phototropin 1 Receptor Kinase Activation and Endocytosis by Blue Light. *The Plant Cell* **21**, 3226–3244 (2009).

198. Roberts, D. *et al.* Modulation of Phototropic Responsiveness in Arabidopsis through Ubiquitination of Phototropin 1 by the CUL3-Ring E3 Ubiquitin Ligase CRL3NPH3. *The Plant Cell* **23**, 3627–3640 (2011).

199. Łabuz, J. *et al.* Phototropin Interactions with SUMO Proteins. *Plant and Cell Physiology* **62**, 693–707 (2021).

200. Preuten, T., Blackwood, L., Christie, J. M. & Fankhauser, C. Lipid anchoring of A rabidopsis phototropin 1 to assess the functional significance of receptor internalization: should I stay or should I go? *New Phytol* **206**, 1038–1050 (2015).

201. Salomon, M., Zacherl, M. & Rudiger, W. Asymmetric, Blue Light-Dependent Phosphorylation of a 116-Kilodalton Plasma Membrane Protein Can Be Correlated with the First- and Second-Positive Phototropic Curvature of Oat Coleoptiles. *Plant Physiology* **115**, 485–491 (1997).

202. Salomon, M., Zacherl, M. & Rüdiger, W. Phototropism and Protein Phosphorylation in Higher Plants: Unilateral Blue Light Irradiation Generates a Directional Gradient of Protein Phosphorylation Across the Oat Coleoptile. *Botanica Acta* **110**, 214–216 (1997).

203. Motchoulski, A. & Liscum, E. Arabidopsis NPH3: A NPH1 Photoreceptor-Interacting Protein Essential for Phototropism. *Science* **286**, 961–964 (1999).

204. Pedmale, U. V. & Liscum, E. Regulation of Phototropic Signaling in Arabidopsis via Phosphorylation State Changes in the Phototropin 1-interacting Protein NPH3. *Journal of Biological Chemistry* **282**, 19992–20001 (2007).

205. Haga, K., Tsuchida-Mayama, T., Yamada, M. & Sakai, T. Arabidopsis ROOT PHOTOTROPISM2 Contributes to the Adaptation to High-Intensity Light in Phototropic Responses. *The Plant Cell* **27**, 1098–1112 (2015).

206. Sullivan, S., Kharshiing, E., Laird, J., Sakai, T. & Christie, J. M. Deetiolation Enhances Phototropism by Modulating NON-PHOTOTROPIC HYPOCOTYL3 Phosphorylation Status. *Plant Physiology* **180**, 1119–1131 (2019).

207. Christie, J. M., Suetsugu, N., Sullivan, S. & Wada, M. Shining Light on the Function of NPH3/RPT2-Like Proteins in Phototropin Signaling. *Plant Physiology* **176**, 1015–1024 (2018).

208. Kimura, T. *et al.* The Phosphorylation Status of NPH3 Affects Photosensory Adaptation During the Phototropic Response. 2020.12.01.**407205** https://www.biorxiv.org/content/10.1101/2020.12.01.407205v1 (2020).

209. Deng, Z. *et al.* Blue Light-Induced Proteomic Changes in Etiolated Arabidopsis Seedlings. *J. Proteome Res.* **13**, 2524–2533 (2014).

210. Christie, J. M. & Murphy, A. S. Shoot phototropism in higher plants: New light through old concepts. *American Journal of Botany* **100**, 35–46 (2013).

211. Zourelidou, M. *et al.* Auxin efflux by PIN-FORMED proteins is activated by two different protein kinases, D6 PROTEIN KINASE and PINOID. *eLife* **3**, e02860 (2014).

212. Teale, W. D., Paponov, I. A. & Palme, K. Auxin in action: signalling, transport and the control of plant growth and development. *Nat Rev Mol Cell Biol* **7**, 847–859 (2006).

213. Fankhauser, C. & Christie, J. M. Plant Phototropic Growth. *Current Biology* **25**, R384–R389 (2015).

214. Haga, K. & Sakai, T. PIN Auxin Efflux Carriers Are Necessary for Pulse-Induced But Not Continuous Light-Induced Phototropism in Arabidopsis. *Plant Physiology* **160**, 763–776 (2012).

215. Haga, K. & Sakai, T. Differential roles of auxin efflux carrier PIN proteins in hypocotyl phototropism of etiolated Arabidopsis seedlings depend on the direction of light stimulus. *Plant Signaling & Behavior* **8**, e22556 (2013).

216. Ding, Z. *et al.* Light-mediated polarization of the PIN3 auxin transporter for the phototropic response in Arabidopsis. *Nat Cell Biol* **13**, 447–452 (2011).

217. Bontinck, M. *et al.* Recent Trends in Plant Protein Complex Analysis in a Developmental Context. *Frontiers in Plant Science* **9**, 640 (2018).

218. Titeca, K., Lemmens, I., Tavernier, J. & Eyckerman, S. Discovering cellular protein-protein interactions: Technological strategies and opportunities. *Mass Spectrometry Reviews* **38**, 79–111 (2019).

219. Fragkiadaki, A. The role of Arabidopsis thaliana Kin7/Separase complex (KISC) inlight signaling pathways. (University of Crete, 2020).

220. Legris, M. & Boccaccini, A. Stem phototropism toward blue and ultraviolet light. *Physiol Plant* **169**, 357–368 (2020).

221. Goyal, A., Szarzynska, B. & Fankhauser, C. Phototropism: at the crossroads of light-signaling pathways. *Trends in Plant Science* **18**, 393–401 (2013).

222. Sakai, T. & Haga, K. Molecular Genetic Analysis of Phototropism in Arabidopsis. *Plant and Cell Physiology* **53**, 1517–1534 (2012).

223. Folta, K. M. & Spalding, E. P. Unexpected roles for cryptochrome 2 and phototropin revealed by high-resolution analysis of blue light-mediated hypocotyl growth inhibition. *The Plant Journal* **26**, 471–478 (2001).

224. Kong, S.-G. *et al.* Both Phototropin 1 and 2 Localize on the Chloroplast Outer Membrane with Distinct Localization Activity. *Plant and Cell Physiology* **54**, 80–92 (2013).

225. Wan, Y.-L. *et al.* The subcellular localization and blue-light-induced movement of phototropin 1-GFP in etiolated seedlings of Arabidopsis thaliana. *Mol Plant* **1**, 103–117 (2008).

226. Liscum, E. Blue Light-Induced Intracellular Movement of Phototropins: Functional Relevance or Red Herring? *Frontiers in Plant Science* **7**, 827 (2016).

227. Sullivan, S., Kaiserli, E., Tseng, T.-S. & Christie, J. M. Subcellular localization and turnover of Arabidopsis phototropin 1. *Plant Signal Behav* **5**, 184–186 (2010).

228. Horio, T. & Murata, T. The role of dynamic instability in microtubule organization. *Frontiers in Plant Science* **5**, 511 (2014).

229. Knieb, E., Salomon, M. & Rüdiger, W. Autophosphorylation, Electrophoretic Mobility and Immunoreaction of Oat Phototropin 1 Under UV and Blue Light¶. *Photochemistry and Photobiology* **81**, 177–182 (2005).

230. Sakamoto, K. & Briggs, W. R. Cellular and Subcellular Localization of Phototropin 1. *Plant Cell* **14,** 1723–1735 (2002).

231. Zulawski, M., Braginets, R. & Schulze, W. X. PhosPhAt goes kinases--searchable protein kinase target information in the plant phosphorylation site database PhosPhAt. *Nucleic Acids Res* **41**, D1176-1184 (2013).

232. Franklin, K. A. Photomorphogenesis: Plants Feel Blue in the Shade. *Current Biology* **26**, R1275–R1276 (2016).

233. Sadegh, S., Higgins, J. L., Mannion, P. C., Tamkun, M. M. & Krapf, D. Plasma Membrane is Compartmentalized by a Self-Similar Cortical Actin Meshwork. *Phys Rev X* **7**, 011031 (2017).

234. Olmsted, Z. T., Colliver, A. G., Riehlman, T. D. & Paluh, J. L. Kinesin-14 and kinesin-5 antagonistically regulate microtubule nucleation by γ-TuRC in yeast and human cells. *Nat Commun* **5**, 5339 (2014).

235. Nishi, H., Shaytan, A. & Panchenko, A. R. Physicochemical mechanisms of protein regulation by phosphorylation. *Frontiers in Genetics* **5**, 270 (2014).

236. Kodama, Y. & Hu, C.-D. Bimolecular fluorescence complementation (BiFC): A 5-year update and future perspectives. *BioTechniques* **53**, 285–298 (2012).

237. Han, Y. H., Moon, H. J., You, B. R. & Park, W. H. The effect of MG132, a proteasome inhibitor on HeLa cells in relation to cell growth, reactive oxygen species and GSH. *Oncol Rep* **22**, 215–221 (2009).

Appendix

Materials and methods

Plant Materials and Growth conditions

The following genotypes of *Arabidopsis thaliana* were used for physiological experiments: the wild type (Col-0), *k135*[135], *phot1-5*, *phot2-1, phot1-5 phot2-1*[238], *nph3* (SALK_122544C) (NASC, England). The light signaling mutants and lines were offered by Dr J. Christie's lab, University of Glasgow. Previous work in Dr. Moschou's lab resulted in generating crosses αTub-GFP/*K135* (lab in Sweden) and PHOT1-GFP/*K135* (Fragkiadaki[219]),which I further characterized by genotyping (see primer sequence in Supplements, S2A). All *Arabidopsis thaliana* lines were grown in a photostable growth chamber (FITOCLIMA 1.200; Aralab) (22°C, 66 ± 1% rH, 16h photoperiod), either on vertical plates containing half strength Murashige and Skoog medium (MS) (Duchefa, Netherlands), supplemented with 1% (w/v) sucrose and 0.8% (w/v) plant agar, or in canna terra soil. Light emitting diodes (LED) and flashlight emitting BL in low output (at the specific intensities described in the result section) were incorporated in growth chamber and used for the BL physiological experiments. *N. benthamiana* plants were grown in a photostable growth chamber (FITOCLIMA 1.200; Aralab) (22o C, 66 ± 1% rH, 16h photoperiod).

Molecular Biology experiments

Full-length NtGR-RBP1 into a pENTR/DTopo vector (Invitrogen, Carlsbad, CA) was subcloned into gateway-compatible pB7WGF2.0 (for N-terminal tag-GFP)[239] (for localization studies), pGAT4 (for protein expression in bacteria) and G1 (gene expression, designed in Dr. Moschou's lab)–by LR recombination with LR Clonase (Thermofisher, Waltham, MA). The entry clones were then subcloned to gateway destination vectors as above. PTB3 and PSP constructs were already available in Dr. Moschou lab. TAP-construct for PHOT1 from Kin7.3 was ordered from ABRC, with stock number AT3G45780.1 for the order (more details in Fragkiadaki[219]).

Site-directed mutagenesis for RBP1 and Kin7.3 point mutants was performed by reverse pcr using Phusion High Fidelity DNA Taq polymerase(New England Biolabs, Ipswich, ES) and DpnI (New England Biolabs) digestion as described by Forloni et al.[240] on entry vectors (pENTR/DTopo for RBP1 constructs) and pZEO (for Kin7.3 constructs). Same mutagenesis pipeline was followed for RBP1^{Y114F} and RBP1^{Y129F}, which were subcloned into gateway-compatible pB7WGF2,0. and G1 by LR recombination. All vectors were transformed into *E.Coli* DH5a strain for propagation and storage. For protein expression in bacteria, constructs were transformed in BL21 cells. Genotyping PCR was performed following the Edwards protocol using Taq polymerase (Enzyquest, Greece) and primers provided in Supplements.

Agroinfiltration-Transient expression in N. benthamiana

A. tumefaciens strain GV3101 was transformed with RBP1, RBP1^{K55R}, RBP1^{Y114F} RBP1^{Y129F} (in pB7WGF2.0, rif^R, spec^R, gent^R), RBP1, RBP1^{K55R} (in G1, rif^R, spec^R, gent^R), PTB3 (in G1, rif^R, spec^R, gent^R), GRP7 (in G1, rif^R, spec^R, gent^R) and PSP (in G6, for N-terminal GFP tag and C-terminal RFP tag, rif^R, spec^R, gent^R). Agrobacteria cultures were inoculated into YEP medium (16-20h, 28°C, darkness), pelleted by centrifugation (2000xg, 3min, 4°C), resuspended in 2x infiltration buffer (MES 10mM, MgCl2 10mM, Acetosyringone 200µM) for 2h and infiltrated into the top leaves of *N. benthamiana*. All constructs were co-infiltrated with P19 (rif^R, kan^R) in order to suppress gene silencing[241], adjusted to optical density (OD_{600}) 0.4. *Agrobacterium* infiltration (agroinfiltration) was performed as previously described by Ruiz et al.[242] *N. benthamiana* plants were grown in a photostable growth chamber (FITOCLIMA 1.200; Aralab) (22o C, 66 ± 1% rH, 16h photoperiod). Expression of proteins was visualized at 3-4 days after infiltration.

Confocal imaging and image analysis

For fluorescence microscopy of Arabidopsis 35:PHOT1-GFP, 35:PHOT1-GFP/*k135,* αTub-GFP and αTub-GFP*/k135* were surface sterilized by bleach and stratified seedlings were grown in the dark for 4 days before imaging observation. Dark grown seedlings were then mounted in water under coverslip and exposed to BL laser irradiation for GFP excitation (488 nm). Images were captured in time course. All samples were imaged though a 40x or 63x oil immersion lens using CLSM Leica SP8 confocal inverted microscope.

For confocal images of transient expression assays, CLSM Leica SP8 confocal inverted microscope was used with 40x and 63x oil immersion lens, adjusting to GFP (488 nm) and RFP (588nm) excitation laser. For heat and cold stress treatments, *N. benthamiana* plants were subjected either to heat (37oC, 30min) or cold (4oC, 30min). Image analyses and intensity measurements were done using Fiji[243]. For ratiometric analysis, CTCF [CTCF=Integrated Density – (Area of selected cellx Mean Fluorescence of background readings] ratio of RFP to GFP signal was calculated per same region of interest (ROI) (individual cell). For every image, three ROIs were selected and measured in parallel with three areas lacking signal (background readings), providing a mean value of fluorescence background.

Measurement of Curvature

For phototropism experiments, seedlings were grown on 0.8% agar plates containing 1/2 MS (pH 5.7) supplemented with 0.5% sucrose. After stratification[244], treated with red light (105 µmol m^{-2} s^{-1}, 2h, 22°C) to induce uniform germination and plates were kept in darkness in a vertical position at 22°C for 3 days. Etiolated seedlings were then irradiated with a unilateral blue light-emitting diode source (470nm; 0.1 µmol m^{-2} s^{-1}) for 8h at 22°C. Pictures were captured using a digital camera (D3500; Nikon) and analyzed. phototropic curvature was estimated as “deviation from the vertical hypocotyl growth” measured by ImageJ software, Fiji[243], as described by Christie et al.[238]

Hypocotyl growth inhibition and statistical analysis

Hypocotyl growth inhibition was measured by planting sterilized seeds onto Petri dishes and stratifying them for 48h. After stratification, seeds were treated with red light (105 µmol m^{-2} s^{-1}) for 2h at 22°C to induce uniform germination. Two copies of plates were then kept in absolute dark in a vertical position at 22°C for 3-4 days. At t_{0min}, pictures were taken using a digital camera (D3500; Nikon) of both plates and then one plate continued to grow in the dark and the other was kept under irradiation using a blue light-emitting diode source (470nm; 1 µmol m^{-2} s^{-1}) for 4 hours, when pictures were taken again. To quantify relative hypocotyl growth inhibition, the length of hypocotyls was measured using Fiji (Image J)[243] and hypocotyl growth rates were calculated for dark versus light.

Immunoblot Analyses

For direct detection of proteins from plant material, 3-4 day grown ~10 seedlings per sample were treated with blue light and grinded immediately with 4x Laemmli Sample Buffer [5.8 mM Tris-HCl, pH 6.8, 2.1% SDS, 26.3% (w/v) glycerol, 0.01% bromophenol blue]. Afterwards, samples were boiled for 5 min and centrifuged at 8000g for 5 min. The supernatants were run on 8% SDS-PAGE gel and further and blotted on a PVDF membrane for Western blot. Anti-GFP antibodies (Thermofisher) were blotted on the membrane at a dilution of 1:2000 o/n at 4°C. After 3 washes with Phosphate Buffered Saline (PBS), the blot was incubated with second antibody (anti-rabbit, 1:10000) for 1h and then washed 3 times with PBS. Protein immunodetection of the membrane was performed using Clarity ECL Western Blotting Substrates kit (BIO-RAD, Hercules, CA) and Sapphire Biomolecular Imager (Azure Biosystems, Ireland). Following development, membranes were staining with Coomassie Brilliant Blue stain (CBB) to visualize total proteins as loading control.

Protein Purification and SDS-PAGE analysis

pGAT4 constructs containing RBP1 and $RBP1^{K55R}$ (in pGAT4) were transformed in BL21 (DE3) Rosetta or BL21 (DE3) cells (Sigma-Aldrich, St. Louis, MO). Bacterial cultures were grown in 5 mL of Luria Broth (LB) medium (37°C, o/n), resuspended in LB and inoculated (37°C, 3h), supplemented with 100 mg/L of ampicillin and 25 mg/L of chloramphenicol. Protein expression was induced at OD_{600} 0.5 with 0.1 IPTG (28 °C, 3h), cells were harvested by centrifugation at 2.500xg for 20 min at RT and frozen overnight at -80°C. Pelleted bacterial cultures were resuspended in Lysis Buffer (Triton 0,1%, 20mM Tris-Cl pH 7.5, one tablet of protease inhibitor cocktail (Sigma-Aldrich)), lysed by sonication (5x 30s On, 5x 30s Off cycles) and centrifuged (12.500x*g*, 4°C, 30 min). The soluble fraction was incubated with pre-equilibrated Ni-NTA agarose beads (Thermofisher). After incubation, beads were packed into columns and proteins were washed and eluted in increasing concentrations of imidazole. Protein samples from all stages of the purification procedure were separated by SDS-PAGE and stained with Coomassie Brilliant Blue (CBB) stain. Isolated proteins were stored at -80 with 10% glycerol.

In silico prediction and database search

Alignment of full-length Kin7.3, RBP1 and GRP7 was generated with CLUSTALW[112] and visualized with Jalview[245]. Structural model of the RNA-binding domain of NtRBP1 (4C7Q, PDB) was visualized by PyMOL[246]. SUMOylation site prediction was performed with SUMOgo[113], while phase-separation related predictions with Pi-pi predictor[30], CIDER[121] and PONDR[122]. Comparative analysis of amino acid composition was done as described by Powers et al.[247]

In vivo Kin7.3 phosphorylation sites were found following searches in the PhosPhAt 4.0[248] database and the Kin7.3 interactome by mass spectrometry results from Dr. Moschou's lab.

Graphs and statistical analysis

All graphs and statistical analysis were performed using Prism software.[249]

References

238. Christie, J. M. et al. phot1 Inhibition of ABCB19 Primes Lateral Auxin Fluxes in the Shoot Apex Required For Phototropism. *PLOS Biology* **9**, e1001076 (2011).

239. Maier, R., Brandner, C., Hintner, H., Bauer, J. & Onder, K. Construction of a reading frame-independent yeast two-hybrid vector system for site-specific recombinational cloning and protein interaction screening. *Biotechniques* **45**, 235–244 (2008).

240. Forloni, M., Liu, A. Y. & Wajapeyee, N. In Vitro Mutagenesis Using Double-Stranded DNA Templates: Selection of Mutants with DpnI. *Cold Spring Harb Protoc* (2018).

241. Ye, K., Malinina, L. & Patel, D. J. Recognition of small interfering RNA by a viral suppressor of RNA silencing. *Nature* **426**, 874–878 (2003).

242. Ruiz, M. T., Voinnet, O. & Baulcombe, D. C. Initiation and Maintenance of Virus-Induced Gene Silencing. *The Plant Cell* **10**, 937–946 (1998)..

243. Schindelin, J. et al. Fiji: an open-source platform for biological-image analysis. *Nat Methods* **9**, 676–682 (2012).

244. Last, R. L. & Fink, G. R. Tryptophan-Requiring Mutants of the Plant Arabidopsis thaliana. *Science* **240**, 305–310 (1988).

245. Waterhouse, A. M., Procter, J. B., Martin, D. M. A., Clamp, M. & Barton, G. J. Jalview Version 2—a multiple sequence alignment editor and analysis workbench. *Bioinformatics* **25**, 1189–1191 (2009).

249. *Graph Pad software*.

Supplemental figures

A

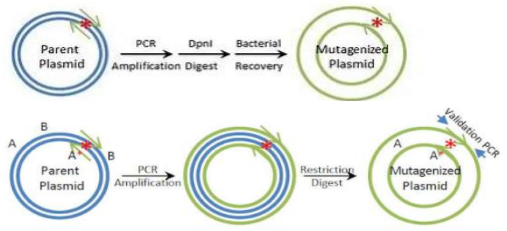

C

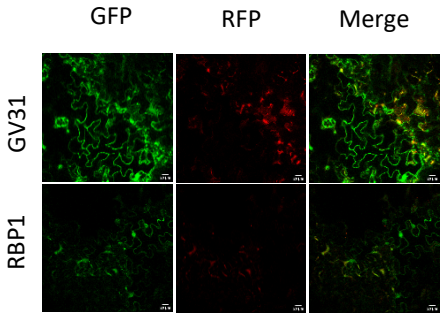

B alternative splicing probe

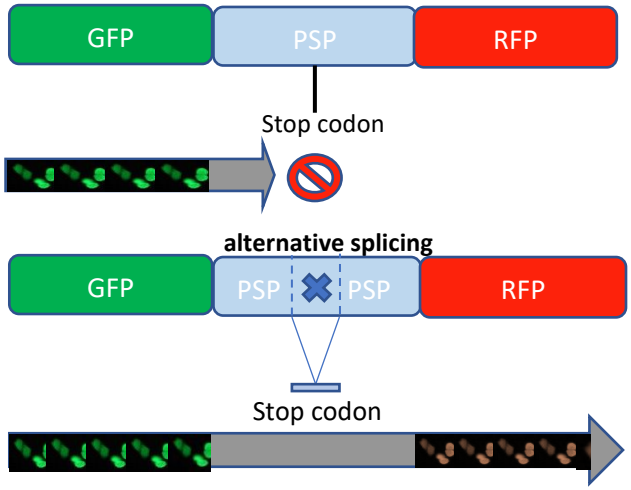

D + alternative splicing probe

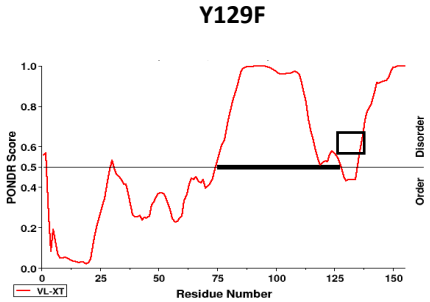

E

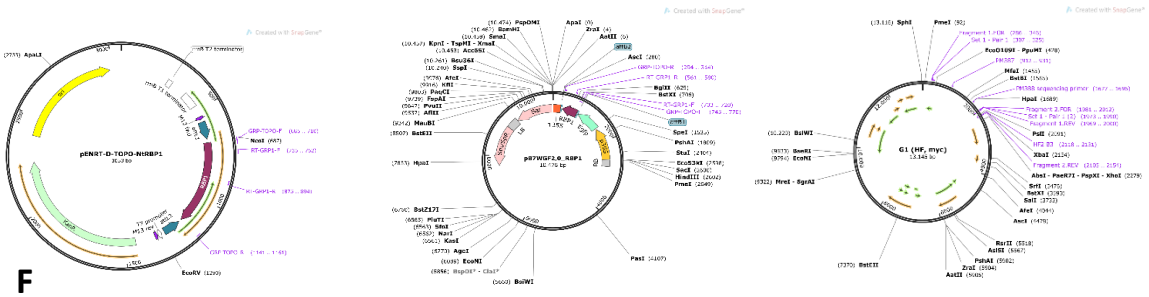

F

Primer	Sequence
K55R top strand	5' TGGATTTGTTACCTTCAGGGATGAGAAAGCCATGA 3'
K55R bottom strand	5' TCATAGGCTTTCTCATCCCTGAAGGTAACAAATCCA 3'
Y114F top strand	5' GAAGGTGGATTCGGTGGTGGCGGCGGTTAC 3'
Y114F bottom strand	5' ACGACGGCCACCACCTC 3'
Y129F top strand	5' AAGGTGGTTTTGGTGGTGGTGGCGGCGGCGGTTATGG 3'
Y129F bottom strand	5' CCATAACCGCCGCCGCCACCACCACCAAAACCACCTT 3'

G

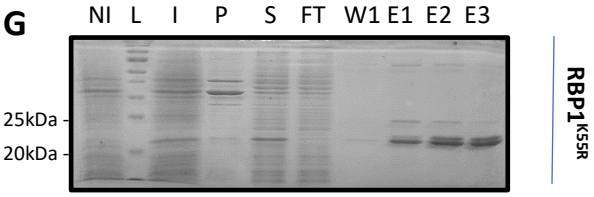

CBB staining

Figure S1. Supplemental figures for Chapter I. (A) DpnI mediated site-directed mutagenesis. Point mutations are introduced to plasmids using overlapping primers harboring the desired mutation in the middle in a PCR protocol that amplifies the entire plasmid template. The parent template is removed using the methylation-dependent endonuclease DpnI and bacteria are transformed with the PCR product. Images and information by Addgene (Watertown, MS), (B) Design of the splicing probe used for ratiometric experiments (Figure 6D). GFP;Gree Fluorescence Protein, RFP; Red Fluorescence Protein, PSP; designated name in Dr. Moschou's lab. When alternative splicing is promoted, exon 2 harboring a stop codon is removed, thereby permitting RFP expression. (C)Respresentative images of ratiometric analysis for GV3101 and RBP1. (D) PONDR prediction for Y129F, Square; disorder-to order transition, (E) Plasmid maps for pENTR/DTOPO_RBP1, pB7WG72,0 (before LR) and G1 (before LR). Visualization by Snapgene (snapgene.com), (F) Primer list for RBP1^{K55R}, RBP1^{Y114F}, Y^{129F}. Primers ordered by invitrogen®, (G) SDS-PAGE analysis of the Ni-NTA purification of RBP1 and RBP1,K55R induction. L; protein ladder, NI;non-induced, I; induced, P;pellet, S;supernatant, FT;flowthrough, W1;wash 1, E1,2,3;elution1,2,3, CBB;Coomasie Brilliant Blue.

A

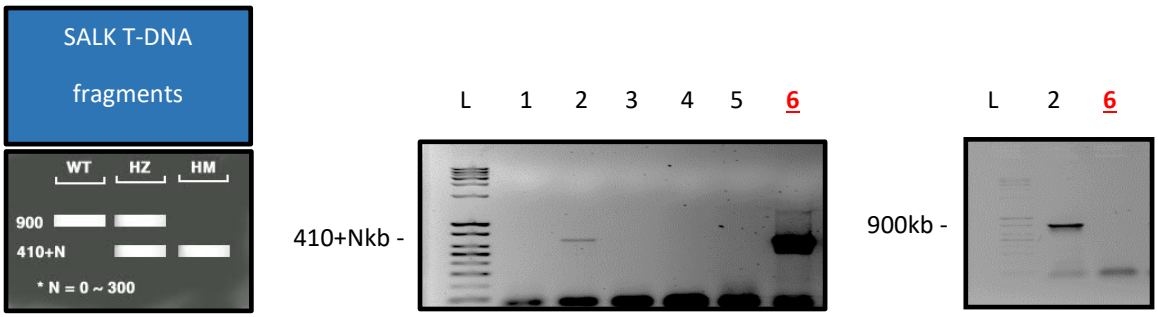

B

T-DNA primers for Kin7.3	**Genomic primers for Kin.7.3**
5' TTTTTGCATTTGTTCCCAGAC 3' **LP**	5' TTTTTGCATTTGTTCCCAGAC 3' **LP**
5' ATTTTGCCGATTTCGGAAC 3' **Lbb1.3**	5' TGAGTGTTTGCTGAATGATGC 3' **RP**

C

Primer	Sequence
S266A top strand	CAGATGAAGCTGCAAAGGCCCCTCAAAATGAGGAG
S266A bottom strand	CTCCTCATTTTGAGGGGCCTTTGCAGCTTCATCTG
S618A top strand	GAGAAGCTTTAGAAGACGCTTCCCATGAAATGGAGA
S618A bottom strand	TCTCCATTTCATGGGAAGCGTCTTCTAAAGCTTCTC
S501A top strand	ATCCGCGGAGGAGACATGCATTTGGGGAAGAAGAG
S501A bottom strand	CTCTTCTTCCCCAAATGGATGTCTCCTCCGCGGAT

D

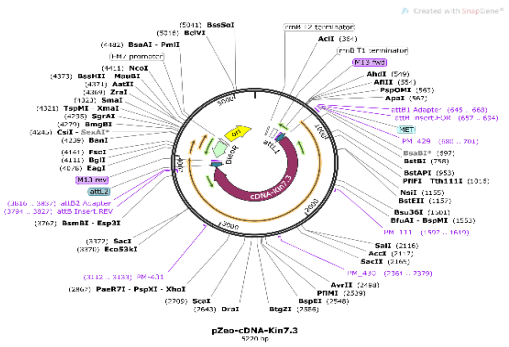

Figure S2. Supplemental figures for Chapter II. (A) Genotyping PCR for k135 background validation. (Left panel) Expected DNA fragment sizes after genotyping PCR. WT; wild-type, HZ; homozygous, HZ; heterozygous,(Middle panel) PCR products resulted from genomic DNA and primer set for T-DNA screening. L;ladder, Numbers 1-6; samples, number 2 and 6 showed T-DNA amplification (Right panel) PCR products resulted from genomic DNA and primer set for genomic DNA screening. DNA template was extracted from Col-0 (wild-type) and k135mutant line.L;ladder, Numbers 2,6; sample 6 is homozygous for loss-of-function Kin7.3, (B) Sets of primers for T-DNA and genomic DNA screening. First screening was performed for T-DNA insertion (left panel) and selected samples were screened for genomic DNA (right panel). Experiment and primers design as described in http://signal.salk.edu/tdnaprimers.2.html. LP;left genomic primer, RP;right genomic primer, Lbb1.3; left DNA border primer. (C)Primer list for Kin7.3 mutants S266A, S618A, and S501A, (D) Plamid map for pZeo_Kin7.3. from Snapgene®.